This is a pre-print of a paper published in the *Journal of Quantitative Spectroscopy and Radiative Transfer* as [JQSRT 312 (2024) 108794]

Generalized Airy Theory and Its Region of Quantitative Validity

James A. Lock[1], Gunther P. Können[2,3], and Philip Laven[4, *]

[1]Physics Dept., Cleveland State University, Cleveland, OH 44115 USA
[2]Sophialaan 4, NL-3761 DK Soest, The Netherlands
[3]deceased 14, Nov. 2022
[4]9 Russells Crescent, Horley, RH6 7DJ, UK
* Corresponding author: philip@philiplaven.com

Abstract:

Airy theory has long proved to be a remarkably simple analytical model that describes the various features of the atmospheric rainbow. But the stringent assumptions upon which its derivation is based, prevent it from being quantitatively accurate in practical situations. We derive an analytical generalization of Airy theory for both the transverse electric and magnetic polarizations and for an arbitrary number of internal reflections. This generalized analytical model contains both the Airy integral and its first derivative, multiplied by constants of proportionality that are independent of the scattering angle. We find that, for the primary rainbow, it provides a quantitatively accurate approximation to the exact Lorenz-Mie-Debye theory of the rainbow for a much wider range of sizes of spherical water drops than does the original version of Airy theory, but still has stringent limitations for the second-order rainbow and beyond.

Key words

Airy theory, analytical generalization

1. Introduction

The rainbow is a both a beautiful and rich physical phenomenon whose theory has been updated and improved many times from the time of Theodoric of Freiberg seven centuries ago, until the present day [1, 2]. Some features of the rainbow which are understood in terms of ray optics, such as its angular position in the sky and its color separation, involved the contributions of a number of researchers, most notably Descartes and Newton [1, 3]. Other features of the rainbow which are understood in terms of wave optics, such as the large-but-finite intensity of the rainbow itself and the supernumerary interference pattern adjacent to it, involved the contributions of a number of later researchers, most notably Young and Airy [1, 3]. In particular, Airy derived an analytical formula for the intensity of the rainbow and its accompanying supernumerary interference pattern using a mixture of ray theory and wave theory for the idealized case of scattering of a monochromatic plane wave of light of wavelength λ by a single spherical water droplet of radius a and real refractive index N [4]. After nearly two centuries, Airy's formula remains brilliant in its simplicity in that it provides a large amount of significant information about the rainbow, starting from only a small number of physical inputs, namely the curvature of the cubic wavefront exiting the sphere in the vicinity of the Descartes rainbow ray and the product of the Fresnel reflection and transmission coefficients of the Descartes ray ([5, 6] and see section 13.23 of [7]).

The present state of the art of the theory of the rainbow for scattering of a monochromatic plane wave by a single spherical water droplet has evolved from ray theory and Airy theory along several different paths. Following the path of development that takes a purely numerical point of view, one can compute the scattered intensity of the exact Lorenz-Mie-Debye theory [7, 8]. Since the geometric optics intensity scales as x^2 (where x is the size parameter defined by $x = 2\pi a/\lambda$) while the intensity of the rainbow for p-1 internal reflections scales as $x^{7/3}$ according to Airy theory, one can numerically watch the rainbow slowly rise above the geometric optics background as x is increased in the numerical computations. In order to make numerical computations more closely reflect observations of rainbows in the natural environment, one can average the scattered intensity over a realistic size distribution of water droplets in a rain shower, over the finite angular width of the sun, and over the wavelengths in the visible part of the solar spectrum.

Following the path of rainbow theory development that takes an analytical point of view, one applies the Complex Angular Momentum (CAM) method to the partial wave sum for each value of p [9 - 14]. This is followed by the Chester-Friedman-Ursell (CFU) uniform approximation in the vicinity of the p-1 order rainbow [11, 15 - 18]. One obtains an analytical formula that expresses the scattered electric field in the rainbow region in terms of both the Airy integral and its first derivative, each of which is multiplied by an infinite series of polarization-dependent and scattering angle-dependent coefficients. The original version of Airy theory is a transitional approximation that is accurate near the Descartes rainbow deflection angle, but becomes increasingly inaccurate as the deflection angle moves farther into the supernumerary region. The CFU version of rainbow theory, on the other hand, remains uniformly accurate from Alexander's dark band, through the main rainbow peak, to deep within the supernumerary interference region.

In spite of these more sophisticated developments in the theory of the rainbow, there continues to be an interest in obtaining an analytic formula for the intensity of the rainbow and its accompanying supernumerary interference pattern that closely approximates the exact results of Lorenz-Mie-Debye theory [19]. The original version of Airy's theory expresses the scattered electric field in the vicinity of the first-order rainbow in terms of what is today called the Airy integral (see Sec. 10.4 of [20]), whose argument depends on only the cubic wavefront parameter h, the sphere size parameter x, and the deviation Δ of the ray deflection angle Θ from the Descartes rainbow ray Θ^R. The Airy integral is multiplied by a constant of proportionality that is independent of Θ and which depends in part on the product of the polarization-dependent flat-interface Fresnel reflection and transmission coefficients evaluated at the angle θ_i^R of the incident Descartes ray. Airy's original formula for the first-order rainbow and the transverse electric polarization (TE) of the incident electromagnetic plane wave has been generalized to TE-polarized light for all higher-order rainbows having $p \geq 3$ [21, 22]. It has also been generalized to incident light with the transverse magnetic (TM) polarization and $p = 2$ [23]. In this case for N

= 1.333, the Brewster angle of incidence of $\theta_i^B = 53.14°$ is close to the angle of incidence of the $p = 2$ Descartes rainbow ray, $\theta_i^R = 59.41°$. The variation in the amplitude of the participating rays along the wavefront produces a contribution to the scattered electric field in the vicinity of the rainbow that is proportional to the first derivative of the Airy integral with respect to its argument. We give the name generalized Airy theory to the extension of Airy's original theory, that takes into account to first order, this amplitude variation of the participating rays. The scattered electric field of generalized Airy theory is equal to the sum of an Airy integral term, plus another term proportional to its first derivative, each multiplied by a polarization-dependent but Θ-independent constant. This inclusion of a first-order amplitude variation produces a much wider region of validity than that of the original version of Airy theory, although it continues to have stringent limits for $p \geq 3$.

Section 2 of this paper describes our terminology and notation. In section 3, we derive generalized Airy theory, beginning from ray theory. In section 4, we determine the range of validity of generalized Airy theory in x-Δ space for arbitrary p and both polarizations of the incident plane wave. Many decades ago, (see p. 246 of [7]) van de Hulst showed that the original version of Airy theory for the TE polarization, $p = 2$ and $N = 1.333$ was expected to be quantitatively accurate only when $x \gtrsim 5{,}000$ (i.e. $a \gtrsim 520$ μm for $\lambda \approx 0.65$ μm). This limitation has been mentioned in almost all subsequent studies of Airy theory [11 - 13]. It is also far above the size at which rain drops begin to become oblate spheroidal as they fall through the air, $a \approx 170$ μm [24, 25] (i.e. $x \approx 1{,}650$ for $\lambda = 0.65$ μm). This limitation of the original version of Airy theory provides only qualitative information, and not quantitative information, about rainbows observed outdoors following a rain shower. A renewed interest in the range of quantitative validity of Airy theory has recently appeared in the literature [26], for which a numerical ray tracing point of view was taken. The present study, which takes an analytical point of view, can be considered as complementary to this.

The analysis of section 4, however, shows that the quantitative applicability of generalized Airy theory extends to size parameters smaller than that of the original version of Airy theory by more than a factor of ten. For the TE polarization, $p = 2$, and $N = 1.333$, generalized Airy theory is quantitatively accurate for $x \gtrsim 360$ (i.e $a \gtrsim 37$ μm at $\lambda = 0.65$ μm) which describes scattering by small spherical water drops that participate in rain showers.

In section 5, we discuss the false Brewster angle artifact present in generalized Airy theory. In section 6, we numerically test the accuracy of generalized Airy theory for TE and TM polarizations with N=1.333 for $p = 2$ and $p = 3$ to determine its validity as a function of droplet size. Section 7 considers some special cases that lie beyond the capabilities of generalized Airy theory, and we propose further improvements to it. Lastly, we present our conclusions in section 8.

2. Terminology and Notation

We start by considering geometrical ray theory for a monochromatic incident electromagnetic plane wave of electric field strength E_0, wavelength λ, wave number $k = 2\pi/\lambda$ and time dependence $\exp(-i\omega t)$, propagating in the $\mathbf{u_z}$ direction and linearly polarized in the $\mathbf{u_x}$ direction. The geometrical rays that comprise the plane wave are scattered by a single homogeneous spherical particle of radius a and real refractive index N, whose center coincides with the origin of a spherical coordinate system (r,θ,φ). The angle of incidence of an incoming ray at the sphere surface is θ_i, its angle of refraction into the sphere is θ_t, and its deflection angle upon exiting the sphere following p-1 internal reflections is Θ. The angles θ_i and θ_t are related by Snell's law, and they are related to Θ by

$$\Theta = (p-1)\,\pi + 2\theta_i - 2p\theta_t \quad . \qquad (2.1)$$

The scattering angle θ of the ray is related to its deflection angle by

$$\theta = \arccos[\cos(\Theta)] \quad . \qquad (2.2)$$

The angles of incidence and transmission of the Descartes rainbow ray making p-1 internal reflections inside the sphere are

$$\cos(\theta_i^R) = [(N^2 - 1)/(p^2 - 1)]^{1/2} \equiv c \qquad (2.3a)$$

$$\sin(\theta_i^R) = [(p^2 - N^2)/(p^2 - 1)]^{1/2} \equiv s \qquad (2.3b)$$

$$\cos(\theta_t^R) = (p/N)\cos(\theta_i^R) \qquad (2.3c)$$

$$\sin(\theta_t^R) = (1/N)\sin(\theta_i^R) \quad , \qquad (2.3d)$$

and its deflection angle is

$$\Theta^R = (p-1)\,\pi + 2\theta_i^R - 2p\theta_t^R \quad . \qquad (2.4)$$

The quantity h describing the cubic shape of the outgoing wavefront in the vicinity of the rainbow ray is given by

$$h \equiv [(p^2 - 1)/p^2]\,(s/c^3) \; . \qquad (2.5)$$

The deflection angle of an arbitrary ray with respect to the Descartes rainbow ray is parameterized by Δ, where

$$\Theta = \Theta^R + \Delta \quad . \qquad (2.6)$$

The rainbow as a function of Δ is a transition from the two-ray supernumerary region $\Delta>0$ where the upper (U) and lower (L) supernumerary rays with different angles of incidence θ_i^U and θ_i^L are deflected in the same direction Θ

$$\Theta = (p-1)\,\pi + 2\theta_i^L - 2p\theta_t^L = (p-1)\,\pi + 2\theta_i^U - 2p\theta_t^U \quad , \qquad (2.7)$$

and the zero-ray region where $\Delta < 0$. When θ_i^U and θ_i^L are in the vicinity of θ_i^R, we let

$$\theta_i^{U/L} = \theta_i^R + \varepsilon^{U/L} \tag{2.8a}$$

$$\theta_t^{U/L} = \theta_t^R + \delta^{U/L} \quad , \tag{2.8b}$$

where ε^U and δ^U are positive, ε^L and δ^L are negative, and $\varepsilon^{U/L}$, $\delta^{U/L}$, Δ are all assumed to be small. Since the angle pairs θ_i^U and θ_t^U of the U ray, θ_i^L and θ_t^L of the L ray, and θ_i^R and θ_t^R of the Descartes rainbow ray each satisfy Snell's law, the angles $\delta^{U/L}$ are functions of $\varepsilon^{U/L}$, respectively, having the Taylor series expansion

$$\delta^{U/L} = J_1\, \varepsilon^{U/L} - J_2\, (\varepsilon^{U/L})^2 - J_3\, (\varepsilon^{U/L})^3 + \mathrm{O}[(\varepsilon^{U/L})^4] \tag{2.9}$$

where

$$J_1 = 1/p \tag{2.10a}$$

$$J_2 = [(p^2 - 1)/(2p^3)]\, [(p^2 - N^2)/(N^2 - 1)]^{1/2} \tag{2.10b}$$

$$J_3 = [(p^2 - 1)/(6p^5)]\, [p^2 + 3(p^2 - N^2)/(N^2 - 1)] \quad . \tag{2.10c}$$

The common deflection angle Θ of Eq. (2.7) for the U and L supernumerary rays is a function of their angle of incidence. Using the J_1, J_2, J_3 terms of Eqs. (2.9)(2.10a-c), the deflection angle has the Taylor series expansion

$$\Delta = K_2\, (\varepsilon^{U/L})^2 + K_3\, (\varepsilon^{U/L})^3 + \mathrm{O}[(\varepsilon^{U/L})^4] \tag{2.11}$$

where

$$K_2 = [(p^2 - 1)/p^2][(p^2 - N^2)/(N^2 - 1)]^{1/2} \tag{2.12a}$$

$$K_3 = [(p^2 - 1)/(3p^4)]\, [p^2 + 3(p^2 - N^2)/(N^2 - 1)] \quad . \tag{2.12b}$$

Equation (2.11) can be inverted to give

$$\varepsilon^{U/L} = \pm\, L_1\, \Delta^{1/2} - L_2\, \Delta + \mathrm{O}(\Delta^{3/2}) \tag{2.13}$$

where

$$L_1 = p\, (N^2 - 1)^{1/4}/[(p^2 - 1)^{1/2}(p^2 - N^2)^{1/4}] \tag{2.14a}$$

$$L_2 = [p^2(N^2 - 1) + 3(p^2 - N^2)]/[6(p^2 - 1)(p^2 - N^2)] \quad , \tag{2.14b}$$

and the $\pm$ in Eq. (2.13) associates +/- with the U/L supernumerary ray.

3. Derivation of Generalized Airy Theory

3.1 Ray Theory

In ray theory, the scattered electric field of the U and L supernumerary rays is [27]

$$\mathbf{E}^{\mathbf{U}}{}_{\mathbf{scatt}}(r,\Theta,\varphi) = G(r,\theta)\exp(\mathrm{i}Q)\exp(\mathrm{i}\pi/2)\exp\{\mathrm{i}x[2pN\cos(\theta_t^U)-2\cos(\theta_i^U)]\}\,x$$
$$\times[\sin(\theta_i^U)\cos(\theta_i^U)]^{1/2}\,\{|[p\cos(\theta_i^U)]/[N\cos(\theta_t^U)]-1|\}^{-1/2}$$
$$\times[-\cos(\varphi)\,F^{TM}(\theta_i^U)\,\mathbf{u_\theta}+\sin(\varphi)\,F^{TE}(\theta_i^U)\,\mathbf{u_\varphi}] \qquad (3.1)$$

and

$$\mathbf{E}^{\mathbf{L}}{}_{\mathbf{scatt}}(r,\Theta,\varphi) = G(r,\theta)\exp(\mathrm{i}Q)\exp(\mathrm{i}\pi)\exp\{\mathrm{i}x[2pN\cos(\theta_t^L)-2\cos(\theta_i^L)]\}\,x$$
$$\times[\sin(\theta_i^L)\cos(\theta_i^L)]^{1/2}\,\{[p\cos(\theta_i^L)]/[N\cos(\theta_t^L)]-1\}^{-1/2}$$
$$\times[-\cos(\varphi)\,F^{TM}(\theta_i^L)\,\mathbf{u_\theta}+\sin(\varphi)\,F^{TE}(\theta_i^L)\,\mathbf{u_\varphi}]\,, \qquad (3.2)$$

where

$$G(r,\theta) = [E_0\exp(\mathrm{i}kr-\mathrm{i}\omega t)/(kr)]\,[2\sin(\theta)]^{-1/2} \qquad (3.3a)$$

$$Q = -p\pi/2 \qquad (3.3b)$$

$$x = ka\ . \qquad (3.3c)$$

In Eqs. (3.1),(3.2) the amplitude of the partial wave reflection and transmission coefficients of the U and L supernumerary rays at the sphere surface is approximated by the real flat-interface electric field Fresnel coefficients for transmission (t_{21} and t_{12}) and reflection (r_{121} and r_{212}), where region 2 is exterior to the sphere and region 1 is the sphere interior. The formulas for the TE and TM versions of these Fresnel coefficients are given, for example in Secs. 1.5.2, 1.5.3 of [28]. We denote the product of the Fresnel coefficients for transmission through the sphere following p-1 internal reflections for the U and L rays and for either the TE or TM polarization by

$$F^{TE}(\theta_i^{U/L}) \equiv [t_{21}{}^{U/L}\,(r_{121}{}^{p-1})^{U/L}\,t_{12}{}^{U/L}]^{(TE)} \qquad (3.4a)$$

$$F^{TM}(\theta_i^{U/L}) \equiv [t_{21}{}^{U/L}\,(r_{121}{}^{p-1})^{U/L}\,t_{12}{}^{U/L}]^{(TM)}\ . \qquad (3.4b)$$

Equations (3.1),(3.2) stress the individual contributions that the U and L supernumerary rays make to the total scattered electric field in the (Θ,φ) direction,

$$\mathbf{E_{scatt}}(r,\Theta,\varphi) = \mathbf{E}^{\mathbf{U}}{}_{\mathbf{scatt}}(r,\Theta,\varphi) + \mathbf{E}^{\mathbf{L}}{}_{\mathbf{scatt}}(r,\Theta,\varphi)\ . \qquad (3.5)$$

They simplify in $\varphi = 0°$ azimuthal plane where the scattered light is entirely TM polarized, and in the $\varphi = 90°$ azimuthal plane where it is entirely TE polarized. These two special cases will be considered in this study.

The two scattered supernumerary fields superpose and interfere at each deflection angle Θ. Sometimes the interference is constructive, sometimes it is destructive, and sometimes it lies between these two limits. We wish to rewrite Eqs. (3.1), (3.2), (3.5) in a form that stresses the character of the interference of the U and L rays for a given Θ, so that it exhibits a collective-effect point of view rather than an individual-contribution point of view. In order to simplify the notation of Eqs. (3.1), (3.2) somewhat, we let $\Phi(\Theta,U)$ and $\Phi(\Theta,L)$ be phase of the U and L supernumerary rays,

$$\Phi(\Theta,U) \equiv 2pN\cos(\theta_t^U) - 2\cos(\theta_i^U) \qquad (3.6a)$$

$$\Phi(\Theta,L) \equiv 2pN\cos(\theta_t^L) - 2\cos(\theta_i^L)\ . \qquad (3.6b)$$

We let the amplitude of the U and L supernumerary rays in the $\varphi = 90°$ and $\varphi = 0°$ azimuthal planes be $A^{TE/TM}(\Theta,U)$ and $A^{TE/TM}(\Theta,L)$, where

$$A^{TE/TM}(\Theta,U) \equiv [\sin(\theta_i^U)\cos(\theta_i^U)]^{1/2}\ \{|[p\cos(\theta_i^U)]/[N\cos(\theta_t^U)] - 1|\}^{-1/2}\ F^{TE/TM}(\theta_i^U) \qquad (3.7a)$$

$$A^{TE/TM}(\Theta,L) \equiv [\sin(\theta_i^L)\cos(\theta_i^L)]^{1/2}\ \{[p\cos(\theta_i^L)]/[N\cos(\theta_t^L)] - 1\}^{-1/2}\ F^{TE/TM}(\theta_i^L) \qquad (3.7b)$$

In addition, we let

$$A_{con}(\Theta) \equiv A^{TE/TM}(\Theta,U) + A^{TE/TM}(\Theta,L) \qquad (3.8a)$$

$$A_{\mathrm{des}}(\Theta) \equiv A^{TE/TM}(\Theta,U) - A^{TE/TM}(\Theta,L)\ . \qquad (3.8b)$$

The explicit Θ dependence of the notation $A^{TE/TM}(\Theta,U)$, $A^{TE/TM}(\Theta,L)$, $\Phi(\Theta,U)$, and $\Phi(\Theta,L)$ is meant to remind the reader that these quantities are functions of the deflection angle Θ, the angles of incidence θ_i^U and θ_i^L, and the transmission angles θ_t^U and θ_t^L of the supernumerary rays corresponding to the deflection angle Θ.

3.2 Generalized Airy Theory Phase

In order to express Eq. (3.5) solely in terms of the deflection angle Θ, or equivalently Δ, and eliminate the dependence on the angles of incidence θ_i^U and θ_i^L, we need to invert Eq. (2.7) so as to obtain $\theta_i^U(\Theta)$ and $\theta_i^L(\Theta)$. This was approximately accomplished for the phases $\Phi(\Theta,U)$ and $\Phi(\Theta,L)$ using a Taylor series expansion evaluated with respect to the rainbow angle R, where the first five nonzero terms were kept,

$$\Phi(\Theta,\ U/L) = \Phi(R) + A\,\Delta \pm B\,\Delta^{3/2} + C\,\Delta^2 \pm E\,\Delta^{5/2} + \mathrm{O}(\Delta^3)\ . \qquad (3.9)$$

Our numerical experimentation shows that the oscillations of the scattered intensity in Airy theory using the A and B terms alone start to drift out of phase with respect to the intensity oscillations predicted by the exact Lorenz-Mie-Debye theory as Δ progresses deeper into the supernumerary region. In order to bring the phase of the Airy theory oscillations in line with the Lorenz-Mie-Debye oscillations, we need to effectively stretch it by including the contribution provided by the additional C and E terms.

An efficient way to calculate the coefficients A, B, C, E is as follows. Consider the quantity

$$D \equiv \mathrm{d}\theta_t/\mathrm{d}\theta_i = \cos(\theta_i)/[N\cos(\theta_t)] \qquad (3.10)$$

and its derivatives with respect to θ_i,

$$D_j \equiv \mathrm{d}^jD/\mathrm{d}\theta_i^{\,j}\ . \qquad (3.11)$$

These derivatives evaluated at R will be symbolically denoted as $D_j(R)$. One treats these entities symbolically throughout the calculation, and explicitly evaluates them only as the final step. This strategy allows one to exploit various important time-saving cancellations that occur between the $D_j(R)$, which would likely not have been noticed in other methods. The first step in our approach is to write the Taylor series expansion of Θ with respect to θ_i, and evaluated at R, in terms of the $D_j(R)$. The result is then inverted to express ε in terms of both powers of $\Delta^{1/2}$ and the $D_j(R)$. We keep terms up to and including $O(\Delta^2)$ in the expansion. Next, we Taylor series expand Φ with respect to θ_i and evaluate it at R. The various derivatives of Φ evaluated at R are also expressed in terms of the $D_j(R)$. Now that everything needed for the calculation has been expressed in terms of the $D_j(R)$, the expansion of ε in terms of powers of $\Delta^{1/2}$ is substituted into the Taylor series expansion of Φ with respect to θ_i. After the appropriate cancellations between the resulting $D_j(R)$ terms have been made, the coefficient B in Eq. (3.9) ends up only depending on $D_1(R)$, the coefficient C only depends on $D_1(R)$, $D_2(R)$, and the coefficient E only depends on $D_1(R)$, $D_2(R)$, $D_3(R)$. Lastly, the $D_j(R)$ are explicitly evaluated, and are substituted in. As a result, the coefficients of Eq. (3.9) were found to be

$$\Phi(R) = 2pN\cos(\theta_t^R) - 2\cos(\theta_i^R) \tag{3.12a}$$

$$A = \sin(\theta_i^R) \tag{3.12b}$$

$$B = (2/3)\, pc^{5/2}/[(N^2-1)s]^{1/2} = (2/3)\, h^{-1/2} \tag{3.12c}$$

$$C = \{[c^3/[12(N^2-1)s^2]\}\, [c^2(2p^2+3) - 3(p^2+1)] \tag{3.12d}$$

$$\begin{aligned} E = p\,\{c/[(N^2-1)s]\}^{3/2}\ &\{[c^2/15]\,[3 + c^2(p^2-3)] \\ &+ [c^2/(20s^2)]\,[c^4\,(14p^2/9 + 2/3) - c^2\,(p^2 + 5/3) + 1]\}\ . \end{aligned} \tag{3.12e}$$

Thus we can define

$$\Phi(\Theta, U/L) \equiv \Phi_{symm}(\Delta) \pm \Phi_{anti}(\Delta) \tag{3.13}$$

where

$$\Phi_{symm}(\Delta) \equiv \Phi(R) + A\,\Delta + C\,\Delta^2 + O(\Delta^3) \tag{3.14a}$$

$$\Phi_{anti}(\Delta) \equiv B\,\Delta^{3/2} + E\,\Delta^{5/2} + O(\Delta^{7/2}) \approx (2/3)(\Delta^{3/2}/h^{1/2})(1 + E\Delta/B)\ . \tag{3.14b}$$

We define the Airy theory phase parameter $\zeta(\Delta)$ by

$$(2/3)\zeta(\Delta)^{3/2} \equiv x\Phi_{anti}(\Delta)\ , \tag{3.15}$$

which can be written in terms of the quantity $\chi(\Delta)$ as

$$\zeta(\Delta) = x^{2/3}\chi(\Delta)\ , \tag{3.16}$$

with

$$\chi(\Delta) \approx (\Delta/h^{1/3})\,[(1 + K_1\Delta + O(\Delta^2)] \tag{3.17}$$

and

$$K_1 = (2/3)(E/B) \quad . \tag{3.18}$$

This approximation for $\zeta(\Delta)$ ignores the higher order terms, beginning with $O(\Delta^2)$ in Eq. (3.17) which would arise from the $O(\Delta^{7/2})$ term of Eq. (3.14b). For $p = 2$, $N = 1.333$, and Δ measured in radians, K_1 in Eq.(3.18) has the numerical value $K_1 = 0.1650$. This differs from the numerical value of $K_1 = 0.2011$, of Eqs. (4.14), (4.19), (A27) in [12], which was also quoted in [13]. The result of [12,13] was presumably obtained using the more involved calculational procedure based solely on Eqs. (2.9) - (2.14). We found that our value of K_1 produces a better fit to the intensity oscillations than does the value quoted in [12, 13]. We determined this by computing both the generalized Airy intensity and the Lorenz-Mie-Debye intensity for $p = 2$, $N = 1.333$, and $x = 1,000$. We then numerically determined the locations of the first 18 sharp intensity minima for each model and best-fit their difference by the form of Eqs. (3.16), (3.17). The linear best-fit gave $K_1 = 0.1547$. We also calculated the scattered intensity in both models for $p = 2$, $N = 1.333$, $x = 10,000$. We then best-fit the locations of the first 41 intensity minima in both models, and found nearly identical results for K_1. Our result of $K_1 = 0.1650$ is larger than the numerically-obtained best-fit by 6.7%, while the result of [12, 13] is larger than it by about 30%.

3.3 Zeroth-Order CFU Uniform Approximation

When Eqs. (3.14a),(3.14b) are substituted into Eqs. (3.1),(3.2), the symmetric phase becomes a common factor, and the magnitude of the scattered electric field vector in the two supernumerary rays region can be written in terms of the new variables as

$$\left|\mathbf{E_{scatt}}(r,\theta,\varphi)\right| = G(r,\theta)\exp(\mathrm{i}Q)\exp(3\mathrm{i}\pi/4)\exp[\mathrm{i}x\Phi_{symm}(\Delta)]\ x$$
$$\times\ \{[A_{con}(\Theta)]\cos[x\Phi_{anti}(\Delta) - \pi/4] + \mathrm{i}\,[A_{des}(\Theta)]\sin[x\Phi_{anti}(\Delta) - \pi/4]\}. \tag{3.19}$$

Here, the notation $\left|\mathbf{E_{scatt}}(r,\theta,\varphi)\right|$ indicates that the magnitude of the scattered electric field vector in these directions still contains both a real part and an imaginary part in the complex plane. With the change of variables of Eq. (3.15), the magnitude of the two-supernumerary-ray scattered electric field vector finally becomes

$$\left|\mathbf{E_{scatt}}(r,\theta,\varphi)\right| = G(r,\theta)\exp(\mathrm{i}Q)\exp(3\mathrm{i}\pi/4)\exp[\mathrm{i}x\Phi_{symm}(\Delta)]\ x$$
$$\times\ \{A_{con}(\Theta)\cos[(2/3)\zeta(\Delta)^{3/2} - \pi/4] + \mathrm{i}\,A_{des}(\Theta)\sin[(2/3)\zeta(\Delta)^{3/2} - \pi/4]\}. \tag{3.20}$$

We recall that Eq. (3.20) is identical to Eqs. (3.1),(3.2),(3.5). But it has now been converted from the sum of the two individual contributions, considered separately, into the form that easily locates the deflection angles Θ for which constructive interference (con) and destructive interference (des) occur.

However, in the vicinity of the Descartes rainbow angle where $\Delta \to 0$, we see that $A_{con}(\Theta)$ diverges as $\Delta^{-1/4}$. Thus, in order incorporate the behavior of the sum of the two supernumerary rays for $\Delta \rightarrow 0$ and for $\Delta >> 0$ into a single expression, we now transfer Eq. (3.20) from the ray representation to the Airy representation. The asymptotic form of the Airy function and its first derivative are

$$\cos[(2/3)\zeta(\Delta)^{3/2} - \pi/4] \leftrightarrow [\pi^{1/2}\zeta(\Delta)^{1/4}]\, \mathrm{Ai}[-\zeta(\Delta)] \qquad (3.21a)$$

$$\sin[(2/3)\, \zeta(\Delta)^{3/2} - \pi/4] \leftrightarrow [\pi^{1/2}\zeta(\Delta)^{-1/4}]\, \mathrm{Ai}'[-\zeta(\Delta)]\ . \qquad (3.21b)$$

The crossover from the ray representation to the Airy representation occurs in the interval $1.1 \lesssim \zeta(\Delta) \lesssim 1.4$. With this change of representation and substituting Eq. (3.17) with the neglect of the $K_1\Delta$ term for the $\zeta(\Delta)^{1/4}$ factors, the magnitude of the two-supernumerary-ray scattered electric field vector becomes

$$|\mathbf{E}_{\mathbf{scatt}}(r,\theta,\varphi)| = G(r,\theta)\exp(\mathrm{i}Q)\exp(3\mathrm{i}\pi/4)\exp[\mathrm{i}x\Phi_{\mathrm{symm}}(\Delta)]\,\pi^{1/2}x^{7/6}\chi(\Delta)^{1/4}$$
$$\times \{A_{con}(\Theta)\,\mathrm{Ai}[-\zeta(\Delta)] + \mathrm{i}\,A_{des}(\Theta)\,\mathrm{Ai}'[-\zeta(\Delta)] / [x^{1/3}\chi(\Delta)^{1/2}]\}. \qquad (3.22)$$

The two ray contributions constructively interfere when $\mathrm{Ai}'^2[-\zeta(\Delta)] = 0$ and $\mathrm{Ai}^2[-\zeta(\Delta)]$ is a relative maximum, and the two contributions destructively interfere when $\mathrm{Ai}^2[-\zeta(\Delta)] = 0$ and $\mathrm{Ai}'^2[-\zeta(\Delta)]$ is a relative maximum. Equation (3.22) is identical to the zeroth-order CFU uniform approximation of [15-18], for which Khare and Nussenzveig [12,13] used the notation

$$p_0(\Delta) = A_{con}(\Theta) \qquad (3.23a)$$

$$q_0(\Delta) = [2/\chi(\Delta)]^{1/2} A_{des}(\Theta)\ , \qquad (3.23b)$$

with p_0 and q_0 considered as real quantities in Eqs. (3.23a),(3.23b).

3.4 Generalized Airy Theory Amplitude

In the small-Δ limit, we now evaluate $A^{TE/TM}(\Theta,U)$ and $A^{TE/TM}(\Theta,L)$ of Eqs. (3.7a), (3.7b) up to the $O(\Delta^{1/2})$ correction to the dominant term for both the TE and TM polarization. There are four contributions, three being polarization-independent and one being polarization-dependent. The three polarization-independent contributions are

$$[\sin(\theta_i^{U/L})\cos(\theta_i^{U/L})]^{1/2} = (sc)^{1/2}\,\{1 \pm (L_1/2)[(c/s)-(s/c)]\,\Delta^{1/2} + O(\Delta)\}\ , \qquad (3.24)$$

$$\{|p\cos(\theta_i^{U/L})/[N\cos(\theta_t^{U/L}) - 1|\}^{-1/2} = |\varepsilon^{U/L}|^{-1/2}\,(c/s)^{1/2}\,[p/(p^2-1)^{1/2}]$$
$$\times \{1 \mp (L_1/4)[(c/s) + (3/p^2)(s/c)]\,\Delta^{1/2} + O(\Delta)\}\ , \qquad (3.25)$$

and

$$|\varepsilon^{U/L}|^{-1/2} = L_1^{-1/2}\Delta^{-1/4}\,[1 \pm (L_2/2L_1)\,\Delta^{1/2} + O(\Delta)]\ . \qquad (3.26)$$

For the polarization-dependent contribution, the first two terms of the Taylor series expansion of the product of the TE and TM Fresnel coefficients about the Descartes rainbow ray are

$$F^{TE}(\theta_i^{U/L}) \approx F^{TE}(\theta_i^{R}) + \varepsilon^{U/L}\, F^{TE\prime}(\theta_i^{R}) \quad (3.27a)$$

$$F^{TM}(\theta_i^{U/L}) \approx F^{TM}(\theta_i^{R}) + \varepsilon^{U/L}\, F^{TM\prime}(\theta_i^{R}) \quad (3.27b)$$

where

$$F^{TE}(\theta_i^{R}) = 4p(p - 1)^{p-1}/(p + 1)^{p+1} \quad (3.28a)$$

$$F^{TM}(\theta_i^{R}) = 4pN^2(p - N^2)^{p-1}/(p + N^2)^{p+1} \quad (3.28b)$$

$$F^{TE\prime}(\theta_i^{R}) \equiv (\mathrm{d}F^{TE}/\mathrm{d}\theta_i)_R = F^{TE}(\theta_i^{R})\, h \cos^2(\theta_i^{R}) \quad (3.28c)$$

$$F^{TM\prime}(\theta_i^{R}) \equiv (\mathrm{d}F^{TM}/\mathrm{d}\theta_i)_R = F^{TM}(\theta_i^{R})\, h \cos^2(\theta_i^{R})\, (2p^2N^2 - p^2 - N^4)/(p^2 - N^4) \quad (3.28d)$$

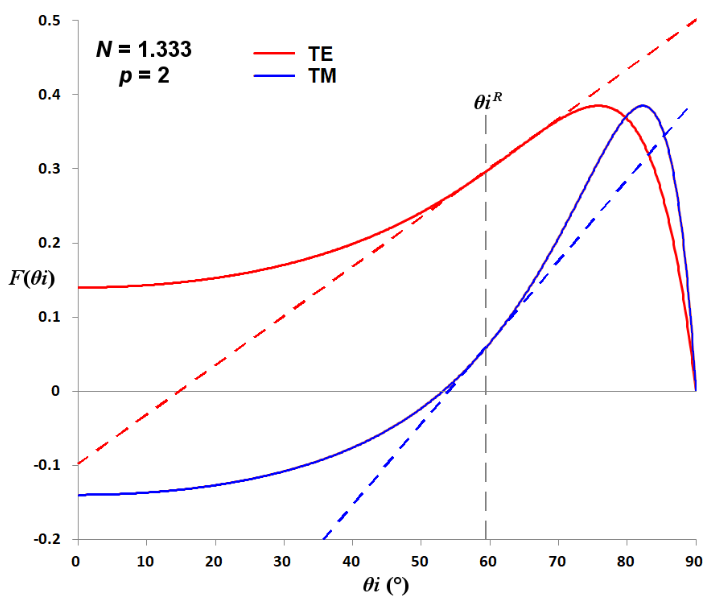

Fig.1. Product of the TE and TM flat interface Fresnel coefficients as a function of the ray angle of incidence, $F^{TE}(\theta_i)$ and $F^{TM}(\theta_i)$, for transmission through a sphere following one internal reflection for $N = 1.333$. The tangent to the curves at the angle of incidence of the Descartes rainbow ray, $\theta_i^R = 59.41°$, is also shown.

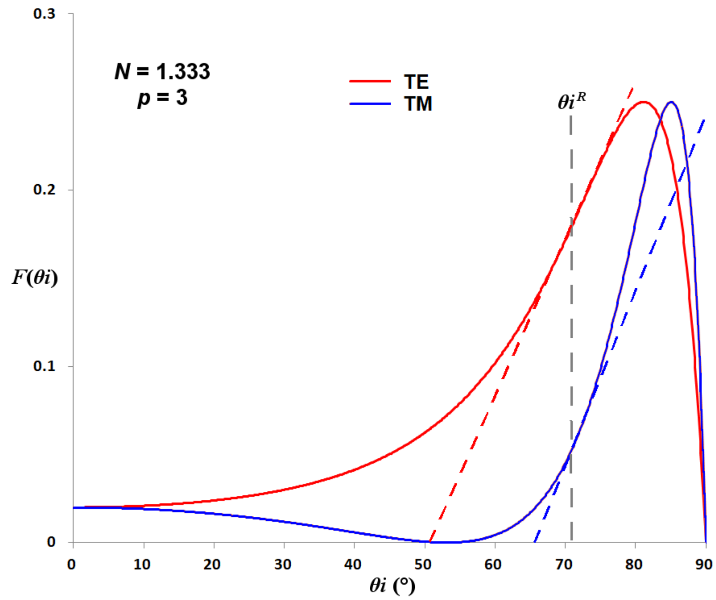

Fig.2. Product of the TE and TM flat interface Fresnel coefficients as a function of the ray angle of incidence, $F^{TE}(\theta_i)$ and $F^{TM}(\theta_i)$, for transmission through a sphere following two internal reflections for $N = 1.333$. The tangent to the curves at the angle of incidence of the Descartes rainbow ray, $\theta_i^R = 71.84°$, is also shown.

One might have thought that modeling the amplitude variation of the outgoing wavefront to higher than first-order would easily lead to a further more accurate generalization of Airy theory. Figures 1 and 2 suggest that this is not so easily accomplished. The product of the Fresnel coefficients, $F^{TE}(\theta_i)$ and $F^{TM}(\theta_i)$, has a sharp relative maximum for large θ_i, and then rapidly decreases to zero as $\theta_i \rightarrow 90°$. This is due to the opposing tendencies of the Fresnel reflection coefficient to approach unity as $\theta_i \rightarrow 90°$ and the Fresnel transmission coefficient to approach zero in the same limit. As a result, many terms in the Taylor series expansion of the product of Fresnel coefficients with respect to the Descartes rainbow ray would be required in order to accurately model this rapid variation occurring far from the Descartes ray. In addition, it was found by numerical experimentation that the Taylor series expansion of $F^{TE}(\theta_i)$ and $F^{TM}(\theta_i)$ for $p = 2, 3$ diverges for $\theta_i << \theta_i^R$ since the magnitude of the Taylor series coefficients increases, rather than decreases, as the term order increases. For these reasons, we limited ourselves to the first-order amplitude modeling. Unfortunately, truncating the product of the Fresnel coefficients by Eqs. (3.27a),(3.27b) will introduce an artifact into the calculated scattered electric field which we call a false Brewster angle effect, and which will be described in detail in section 5.

These four O($\Delta^{1/2}$) contributions to $A^{TE/TM}(\Theta,U)$ and $A^{TE/TM}(\Theta,L)$ are then added and subtracted to form $A_{con}(\Theta)$ and $A_{des}(\Theta)$, which are then substituted into Eq. (3.22) to give the scattered electric field in the supernumerary region as

$$|\mathbf{E}_{\mathbf{scatt}}(r,\Theta,\varphi)| \approx G(r,\theta)\exp(\mathrm{i}Q)\exp(\mathrm{i}L)\exp(\mathrm{i}3\pi/4)\, x^{7/6}\,[(2\pi s)^{1/2}/\,h^{1/3}]$$
$$\times F^{TE/TM}(\theta_i^R)\,\{\mathrm{Ai}[-\zeta(\Delta)] + \mathrm{i}\,h^{1/6}M^{TE/TM}\,\mathrm{Ai}'[-\zeta(\Delta)]/\,x^{1/3}\} \quad , \qquad (3.29)$$

where

$$M^{TE} = [2p^2 - (9\text{-}p^2)\,s^2]/[6p\,(p^2 - 1)^{1/2}\,c^{1/2}\,s^{3/2}] \qquad (3.30\text{a})$$

$$M^{TM} = \{[2p^2 - (9\text{-}p^2)\,s^2](p^2 - N^4) + 12[p(p^2 - 1)\,c\,s]^2\}$$
$$/\,[6p\,(p^2 - 1)^{1/2}\,(p^2 - N^4)\,c^{1/2}\,s^{3/2}] \qquad (3.30\text{b})$$

Equations (3.18),(3.29), (3.30a), (3.30b) are our final equations of generalized Airy theory of the p-1 order rainbow for either the TE or TM polarization. The coefficients of the Airy function and its first derivative are constants, independent of Δ. The original version of Airy theory is described by the same equations, but only with the terms proportional to Ai(-ζ) present. The fact that the terms multiplying both Ai(-ζ) and Ai′(-ζ) in generalized Airy theory are constants, rather than functions of Δ, as is the case in the CFU uniform approximation, allows this theory to retain the simplicity enjoyed by the original version of Airy theory. Since the amplitude variation along the outgoing wavefront in Eqs. (3.24) - (3.27) has been considered here to first order only, it can thus be thought of as being intermediate in sophistication between the original version of Airy theory and the zeroth-order CFU uniform approximation.

4. Region of Validity of Generalized Airy Theory

In this section, we determine when Eqs. (3.18), (3.29), (3.30a), (3.30b) can be expected to be a quantitatively accurate approximation to the exact results of Lorenz-Mie-Debye theory. The criteria we apply here all possess some degree of quantitative arbitrariness. Although the specific values we choose for the arbitrary parameters below are reasonable, other researchers may prefer different values for them. Nonetheless, the conclusions drawn in this section provide a general qualitative estimate for when generalized Airy theory is expected to be quantitatively accurate.

4.1 van de Hulst's Criterion

A size-dependent assumption that will limit the quantitative range of validity of generalized Airy theory in x-Δ parameter space was first considered by van de Hulst in Sec. 13.24 of [7], namely that the interference of the U and L supernumerary rays be able to resolve the principal rainbow peak. van de Hulst applied this criterion to the original version of Airy theory for the TE polarization, $p = 2$, and $N = 1.333$. He found that the original version of Airy theory is a quantitatively accurate approximation only for $x \gtrsim 5{,}000$. van de Hulst's argument is fully reproduced here, since some of the details involved did not explicitly appear in [7]. The original version of Airy theory assumes that the product of the Fresnel coefficients $F^{TE}(\theta_i)$ is constant, having the value $F^{TE}(\theta_i^R)$, in the angle of incidence interval that participates in rainbow formation. He arbitrarily allowed up to a ±10% variation of $F^{TE}(\theta_i)$ from $F^{TE}(\theta i^R)$. This corresponds to the angle of incidence interval

$$\sin(\theta_i^L) = 0.82 \lesssim \sin(\theta_i) \lesssim 0.90 = \sin(\theta_i^U) \ , \tag{4.1}$$

or

$$\theta_i^L = 55° \lesssim \theta_i \lesssim 64° = \theta_i^U \ . \tag{4.2}$$

This range of incident angles produces a deflection angle interval of

$$0° \leq \Delta \lesssim \Delta^{max} = 0.5° \ , \tag{4.3}$$

with $\Delta = 0°$ resulting from θ_i^R, and Δ^{max} resulting from θ_i^L and θ_i^U. In the spirit of Rayleigh's criterion for resolvability of two neighboring point sources (see Secs. 7.6.3 and 8.6.2 of [28]), this deflection angle interval is assumed to be large enough so that the principal rainbow peak can be "just resolved". We know that Ai(-1.0188) = 0.53566 describes the principal rainbow peak, which we denote in what follows by the subscript (0), and Ai(-1.5) = 0.46426 describes the point beyond the principal rainbow peak where the Airy intensity has fallen to 75% of its peak value, i.e.

$$[\mathrm{Ai}(-1.5)/\mathrm{Ai}(-1.0188)]^2 = 0.75 \ . \tag{4.4}$$

This means that the main rainbow peak occurs at

$$\Delta_0 = (1.0188/1.5)\Delta^{max} \approx 20 \text{ minutes of arc} \ . \tag{4.5}$$

Thus, van de Hulst's criterion for the validity of the original version of Airy theory is

$$x^{2/3}\Delta^{max}/h^{1/3} \gtrsim 1.5 \ , \tag{4.6}$$

which gives $x \gtrsim 5{,}000$.

4.2 Scattering Angle Criterion

Another approximation that will limit the region of quantitative validity of generalized Airy theory is that the variation of $F^{TE}(\theta_i)$ and $F^{TM}(\theta_i)$ in the vicinity of θ_i^R be linear, as was assumed in Eqs. (3.27a),(3.27b). The criterion we propose for this is

$$\left|[F^{TE/TM}(\theta_i) - F^{TE/TM}(\theta_i^R) - \varepsilon\, F^{TE/TM\prime}(\theta_i^R)]/F^{TE/TM}(\theta_i)\right| \leq \alpha \tag{4.7}$$

where $\alpha << 1$. We arbitrarily choose $\alpha = 0.05$, which permits up to a ±5% deviation from linearity, which is half the maximum deviation considered in Sec. 3.1 by van de Hulst for the validity of the original version of Airy theory. It should be noted that Eq. (4.7) is independent of ka, except that the flat-surface Fresnel coefficients, upon which Eq. (4.7) is based, require ka >>

1. For $N = 1.333$, and converting the angle of incidence interval to a corresponding deflection angle interval, the maximum value of Δ permitted by Eq. (4.7), Δ^{max}, is given in Table 1.

Table 1

Maximum deflection angle Δ^{max} (measured from Θ^R) corresponding to $\alpha = 0.05$ in Eq. 4.7 for $N = 1.333$ and different values of p.

p	Δ^{max} for TE	Δ^{max} for TM
2	2.89°	0.47°
3	2.40°	0.16°
4	1.80°	0.14°
5	1.54°	0.11°

The region of linearity for the TE polarization is much larger than that for the TM polarization, reflecting the larger curvature of the $F^{TM}(\theta_i)$ graph in the vicinity of θ_i^R.

4.3 van de Hulst's Criterion Revisited

If van de Hulst's criterion for the resolvability of the main rainbow peak of Eq. (4.6) is applied to generalized Airy theory for the TE polarization of the $p = 2$ rainbow for the refractive index $N = 1.333$, we find that $x \gtrsim 360$ when $\Delta^{max} = 2.89°$ as in Table 1. This is more than a factor of 10 below the threshold value of the size parameter for the validity of the original version of Airy theory. As expected from Table 1, the minimum size parameter for the validity of generalized Airy theory increases both as p increases and for the TM polarization. For example, for the TE polarization, $p = 3, 4, 5$, $N = 1.333$, and the value of Δ^{max} given in Table 1, Eq. (4.6) gives $x \gtrsim$ 1,130, 2,900, 5,300, respectively. Also, for the TM polarization, $p = 2$, $N = 1.333$, and the value of Δ^{max} from Table 1, Eq. (4.6) gives $x \gtrsim 5{,}500$, which continue to pose stringent limits on the applicability of generalized Airy theory for $p \geq 3$. We should also note that the consequences of a number of other approximations that were made in the derivation of ray theory from Lorenz-Mie-Debye theory and then generalized Airy theory from ray theory were also examined. It was found that none of them were more restrictive for the values of x and Δ than were the consequences described in sections 4.2 and 4.3.

In spite of this presumed limitation on the original version of Airy theory, in [21] it had been found by numerical experimentation that its comparison to the exact results of Lorenz-Mie-Debye theory was "still surprisingly good" for the TE polarization, $p = 2$, $N = 1.333$, and a size parameter as low as $x = 1{,}933$ or even $x = 483$. The reason for this is now clear. The scattered intensity of generalized Airy theory (GA) for the TM and TE polarizations obtained from Eq. (3.29) is of the form

$$I_{GA}(r,\theta,\varphi{=}0°) \approx C^{TM} \{[\mathrm{Ai}^2[-\zeta(\Delta)] + h^{1/3} (M^{TM})^2 \mathrm{Ai}'^2[(-\zeta(\Delta)] / x^{2/3}\} \ , \quad (4.8a)$$

$$I_{GA}(r,\theta,\varphi{=}90°) \approx C^{TE} \{[\mathrm{Ai}^2[-\zeta(\Delta)] + h^{1/3} (M^{TE})^2 \mathrm{Ai}'^2[(-\zeta(\Delta)] / x^{2/3}\} \ , \quad (4.8b)$$

where C^{TM} *and* C^{TE} are constants. Since $\mathrm{Ai}'^2(-\zeta) = 0$ at a relative maximum of $\mathrm{Ai}^2(-\zeta)$, the scattered intensity in the vicinity of the supernumerary relative maxima is dominated by the $\mathrm{Ai}^2(-\zeta)$ term. Similarly, since $\mathrm{Ai}^2(-\zeta) = 0$ at a relative maximum of $\mathrm{Ai}'^2(-\zeta)$, the scattered intensity in the vicinity of the supernumerary relative minima is dominated by the $\mathrm{Ai}'^2(-\zeta)$ term. This means that when $h^{1/3}\,(M^{TE})^2/x^{2/3} << 1$, the main effect of the $\mathrm{Ai}'^2(-\zeta)$ term on the TE polarized intensity in Eq. (4.8b) is to fill in the zeros of the $\mathrm{Ai}^2(-\zeta)$ term to the appropriate level, and its influence in the vicinity of the supernumerary maxima is negligible. This is the case for $p = 2, 3$, $N = 1.333$, and $x = 483$ since $h^{1/3}\,(M^{TE})^2/x^{2/3} = 0.0037$ and 0.0231, respectively. Thus, it should be no surprise that in spite of the $x = 5{,}000$ limitation of van de Hulst's calculation of the quantitative applicability of the original version of Airy theory, it will still provide a good fit to the locations and heights of the supernumerary maxima for much smaller values of x.

However, when the radius of a spherical falling water drop is greater than about $a \approx 0.17$ mm, it distorts into an oblate spheroid as it falls through the air due to air resistance forces [24, 25]. The aspect ratio of the spheroid gradually increases as a function of a. This produces a small shift in the Descartes rainbow ray scattering angle, known as the Möbius shift, which was calculated for the first-order rainbow over a century ago [29, 30], and was more recently extended to higher-order rainbows in [31, 32]. Furthermore, the angular periodicity of the supernumerary interference pattern has also been found to change as the water drop becomes oblate spheroidal [33, 34]. So, in addition to a minimum size parameter for the quantitative validity of generalized Airy theory, there will also be a nominal maximum size parameter since generalized Airy theory assumes that the falling water droplet remains spherical. For visible light with $\lambda = 0.65$ µm, a rough estimate of the largest size parameter of a falling spherical raindrop is $a \approx 170$ µm, or $x \approx 1{,}643$. According to Eq. (4.6), the minimum size parameter for the validity of generalized Airy theory for the TE polarization, $p = 3$, $N = 1.333$, and the value of Δ^{max} given in Table 1 is $x \gtrsim 1{,}130$. For the TM polarization, $p = 2$, $N = 1.333$, and the value of Δ^{max} from Table 1, Eq. (4.6) gives $x \gtrsim 5{,}500$. Thus, generalized Airy theory can be expected to be a quantitatively accurate approximation to the results of the exact Lorenz-Mie-Debye theory for TE-polarized first and second order rainbows of falling water drops for the nominal size parameter range $360 \lesssim x \lesssim 1{,}643$ and $1{,}130 \lesssim x \lesssim 1{,}643$, respectively when $\lambda = 0.65$µm. On the other hand, since the minimum size parameter for the quantitative accuracy of the TM-polarized $p = 2$ generalized Airy theory is $x = 5{,}500$, it is not guaranteed on the basis of Eq. (4.6) alone that generalized Airy theory will be able to provide a quantitatively accurate approximation for falling spherical raindrops.

Contrary to the situation for generalized Airy theory for the TE polarization, it has been pointed out [12, 13, 23] that since the TM rainbow for $p = 2$ and $N = 1.333$ occurs near the Brewster angle, the $\mathrm{Ai}'^2(-\zeta)$ term in Eqs. (4.8a),(4.8b) will be dominant, and the $\mathrm{Ai}^2(-\zeta)$ term will provide a correction to it. This is easily seen in Eq. (3.29) since for $p = 2$ and $N = 1.333$, one has $h^{1/3}\,(M^{TE})^2 = 0.23$ for the TE polarization, while $h^{1/3}\,(M^{TM})^2 = 127.66$ for the TM polarization, which about 550 times larger. This difference is in part due to the much larger contribution of

$F^{TM\prime}(\theta_i^R)$. Thus the effects of the Ai′(-ζ) term of Eq. (4.8a) for the TM polarization will often be more important than that for the TE polarization. The physical consequences of the Ai′(-ζ) term are numerically studied in detail in sections 5-7 below.

5. False Brewster Angle Artifact

The Brewster angle, Θ^B, in the TM polarization occurs when the internal reflection amplitude vanishes, only the upper supernumerary ray contributes to scattering at Θ^B, and there is no interference pattern. When p is odd, there are an even number of internal reflection coefficients, and the intensity oscillations of the supernumerary interference pattern exhibit a 180° phase shift in the vicinity of Θ^B. On the other hand, when p is even, there are an odd number of internal reflection coefficients and the supernumerary interference pattern exhibits a 0° phase shift in the vicinity of Θ^B. One of the ingredients of generalized Airy theory is that the product of the TE or TM Fresnel coefficients varies linearly in the vicinity of the Descartes rainbow ray,

$$F^{TE}(\theta_i) \approx F^{TE}(\theta_i^R) + F^{TE\prime}(\theta_i^R)\,(\theta_i - \theta_i^R) \qquad (5.1a)$$

$$F^{TM}(\theta_i) \approx F^{TM}(\theta_i^R) + F^{TM\prime}(\theta_i^R)\,(\theta_i - \theta_i^R) \qquad (5.1b)$$

If this linear relationship is assumed to extend to all θ_i, the product of the Fresnel coefficients in Eqs. (5.1a), (5.1b) introduces a potential artifact of a false Brewster angle (*FB*) into both the TE and TM polarizations for generalized Airy at the deflection angle corresponding to

$$\theta_i^{FB,TE} = \theta_i^R - F^{TE}(\theta_i^R)/F^{TE\prime}(\theta_i^R) \qquad (5.2a)$$

$$\theta_i^{FB,TM} = \theta_i^R - F^{TM}(\theta_i^R)/F^{TM\prime}(\theta_i^R) \qquad (5.2b) \quad .$$

The false Brewster angle turns out to pose no special problem for the TE polarization, where Brewster effects should not occur at all, for two reasons. First, it is predicted to occur deep in the supernumerary region, far from the rainbow. For example, for $p = 2$ and $N = 1.333$, $\Theta^R =$ 137.92° and $\Theta^{FB,TE} = 165.93°$, and for $p = 3$, $\Theta^R = 230.92°$ and $\Theta^{FB,TE} = 248.47°$. Second, even when the generalized Airy intensity for the TE polarization is computed in the vicinity of $\Theta^{FB,TE}$, no trace of the false Brewster artifact is seen due to the fact that, in Eqs. (3.24)-(3.28), there are four additive contributions to M^{TE} and M^{TM}. One of them is due to the polarization-dependent product of the Fresnel coefficients, and the other three are independent of polarization. The largest two of these three are opposite in sign to the Fresnel coefficient contribution, and dilute its importance. This is especially true for the TE polarization where for $p = 2$ and $N = 1.333$, M^{TE} would be 1.13 if only the Fresnel coefficient contribution alone was considered. But M^{TE} is reduced by 67.4% to 0.37 when the other three contributions are added. For $p = 3$ and $N = 1.333$, M^{TE} is similarly reduced by 58.5% from 1.65 to 0.68.

The false Brewster angle artifact for the TM polarization is much more problematical for the converse of the two reasons mentioned above for the TE polarization. First, we note that for $p =$ 2 and $N = 1.333$, $\Theta^R = 137.92°$, $\Theta^{FB} = 138.53°$, and $\Theta^B = 138.74°$. For this specific case, the false and true Brewster deflection angles nearly coincide, and so for this reason the false

Brewster artifact should not cause problems. But for $p \geq 3$ and $N = 1.333$ the false Brewster angle remains close to the Descartes rainbow angle, while the true Brewster angle is far from it, causing the false Brewster artifact to severely limit the range of Δ for which generalized Airy theory is accurate. For example, for $p = 3$ and $N = 1.333$, $\Theta^R = 230.89°$, $\Theta^{FB} = 232.64°$, and $\Theta^B = 244.99°$. For $p = 4$ and $N = 1.333$, $\Theta^R = 318.26°$, $\Theta^{FB} = 319.87°$, and $\Theta^B = 351.23°$. Second, the Fresnel coefficient contribution to M^{TM} is significantly larger than it was for the TE polarization. For example, for $p = 2$ and $N = 1.333$ the contribution is 9.43, a factor of 8.4 over what it was for the TE polarization, and for $p = 3$ and $N = 1.333$ it is 5.59, a factor of 3.4 larger than it was for TE. This causes a reduction of the actual value of M^{TM} with all four contributions accounted for by only 8% and 17.2%, respectively, and it continues to be dominated by the polarization-dependent term that contains the false Brewster artifact.

The computed absence of the false Brewster angle artifact for the TE polarization and its presence for the TM polarization in generalized Airy theory can also be understood from another point of view. As is apparent in Fig.10.6 of [20], the maximum value of $\mathrm{Ai}^2(-\zeta)$ slowly decreases as a function of Δ in the supernumerary region, while the maximum value of $\mathrm{Ai}'^2(-\zeta)$ slowly increases. Since the generalized Airy coefficients multiplying these terms are constants, the contribution of the first term in Eq. (4.8a),(4.8b) to the intensity oscillations also decreases throughout the supernumerary region, while the contribution of the second term increases. Let $\langle \mathrm{Ai}^2(-\zeta) \rangle_{\max}$ be the envelope of the relative maxima of $\mathrm{Ai}^2(-\zeta)$, and let $\langle \mathrm{Ai}'^2(-\zeta) \rangle_{\max}$ be the envelope of the relative maxima of $\mathrm{Ai}'^2(-\zeta)$. Then using Eqs. (3.21a),(3.21b),(3.16), these quantities are asymptotically related to each other by

$$\langle \mathrm{Ai}'^2(-\zeta) \rangle_{\max} / \langle \mathrm{Ai}^2(-\zeta) \rangle_{\max} = \zeta \quad . \tag{5.3}$$

As long as

$$\langle \mathrm{Ai}^2(-\zeta) \rangle_{\max} > (h^{1/3} M^2 / x^{2/3}) \langle \mathrm{Ai}'^2(-\zeta) \rangle_{\max} \quad , \tag{5.4}$$

where M is either M^{TE} or M^{TM}, the first term of Eqs. (4.8a),(4.8b) dominates the second term, and the relative maxima of the intensity oscillations coincide with the relative maxima of $\mathrm{Ai}^2(-\zeta)$. But if Δ is deep enough in the supernumerary region so that the inequality switches over to

$$\langle \mathrm{Ai}^2(-\zeta) \rangle_{\max} < (h^{1/3} M^2 / x^{2/3}) \langle \mathrm{Ai}'^2(-\zeta) \rangle_{\max} \quad , \tag{5.5}$$

the second term of Eqs. (4.8a), (4.8b) starts to dominate over the first term, and the relative maxima of the generalized Airy theory intensity oscillations will now coincide with the relative maxima of $\mathrm{Ai}'^2(-\zeta)$. This switchover produces a 180° phase shift in the intensity oscillations centered at

$$\langle \mathrm{Ai}^2(-\zeta) \rangle_{\max} = (h^{1/3} M^2 / x^{2/3}) \langle \mathrm{Ai}'^2(-\zeta) \rangle_{\max} \quad , \tag{5.6}$$

or using Eqs. (3.16), (5.3)

$$\Delta_{180\ phase\ shift} = 1/M^2 \quad . \tag{5.7}$$

This 180° phase shift is associated with the false Brewster angle artifact in generalized Airy theory. For example, for $N = 1.333$ and $p = 2, 3$, one has $(M^{TE})^2 = 0.13$ and 0.47, respectively. Equation (5.7) predicts that any false Brewster angle artifact in the TE polarization would occur many radians away from Θ^R, explaining its absence in the computed results below. But $(M^{TM})^2 =$ 75.17 and 21.43, respectively, leading to $\Delta_{180°\ phase\ shift} = 0.76°$ and 2.67°, respectively, which is in the vicinity of the false Brewster angles corresponding to Eq. (5.2b) having $\Delta_{FB} = 0.61°$ and 1.72°, respectively.

6. Comparisons between calculation methods

Before examining the results of generalized Airy calculations, it is helpful to compare some results of calculations using the original Airy theory and the rigorous Lorenz-Mie-Debye theory, as shown in Figs. 3 and 4. Although the results are similar around the maxima corresponding to the rainbows and their first few supernumerary arcs, the Airy minima have zero intensity. Another problem is that the Airy maxima and minima progressively drift away from their true locations in terms of θ (as discussed in section 3.2): for example, the Airy minimum intensity at $\theta \approx 148.1°$ in Fig. 3 coincides with a Lorenz-Mie-Debye maximum intensity. Note that Figs. 3 and 4 are limited to TE polarization because Airy did not consider TM polarization [4]. Previous sections of this paper have attempted to address all of the above issues by using relatively simple extensions of Airy theory. The rest of this section examines the numerical validity of these extensions for $p = 2$ and $p = 3$ rainbows.

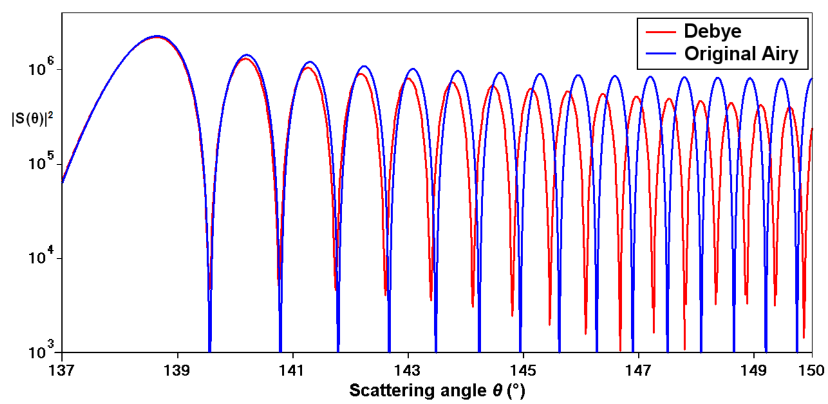

Fig. 3 Scattered intensity as a function of scattering angle for Lorenz-Mie-Debye theory and original Airy theory for TE polarization, $p = 2$, $N = 1.333$, $\lambda = 0.65$ µm, $a = 170$ µm, and $x = 1,643$.

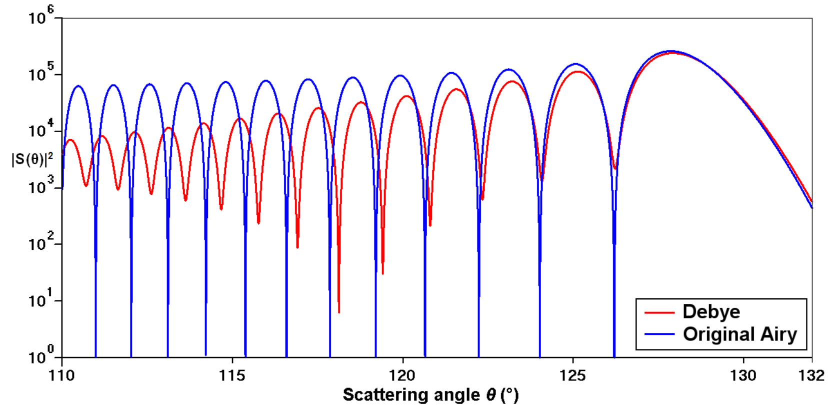

Fig. 4 As Fig. 3 except that $p = 3$.

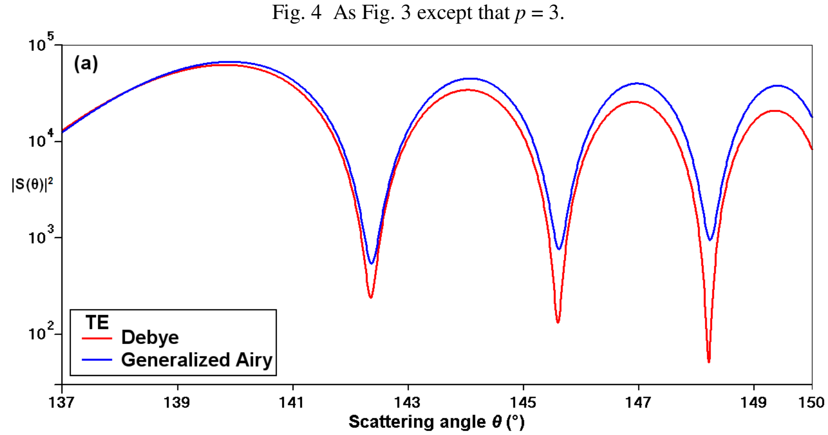

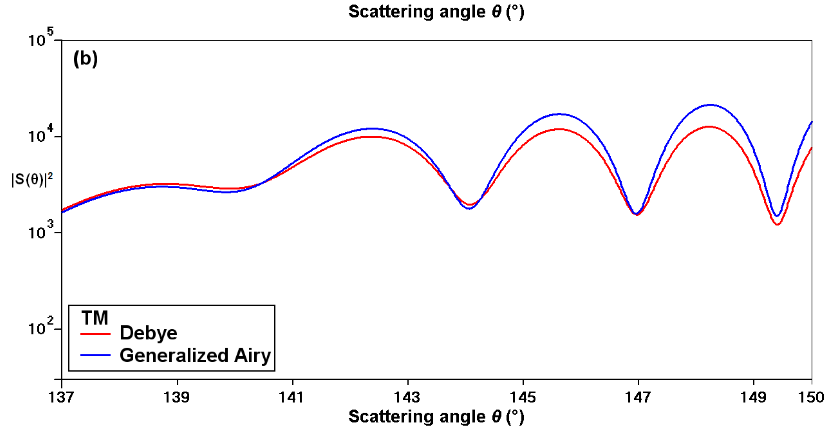

Fig.5 Scattered intensity as a function of scattering angle for Lorenz-Mie-Debye theory and generalized Airy theory of Eq. (3.29) for (a) TE and (b) TM polarizations, $p = 2$, $N = 1.333$, $\lambda = 0.65$ μm, $a = 37.24$ μm, and $x = 360$. This is the smallest size parameter for which Eq. (4.6) predicts that generalized Airy theory is a valid approximation to Lorenz-Mie-Debye theory for the TE polarization.

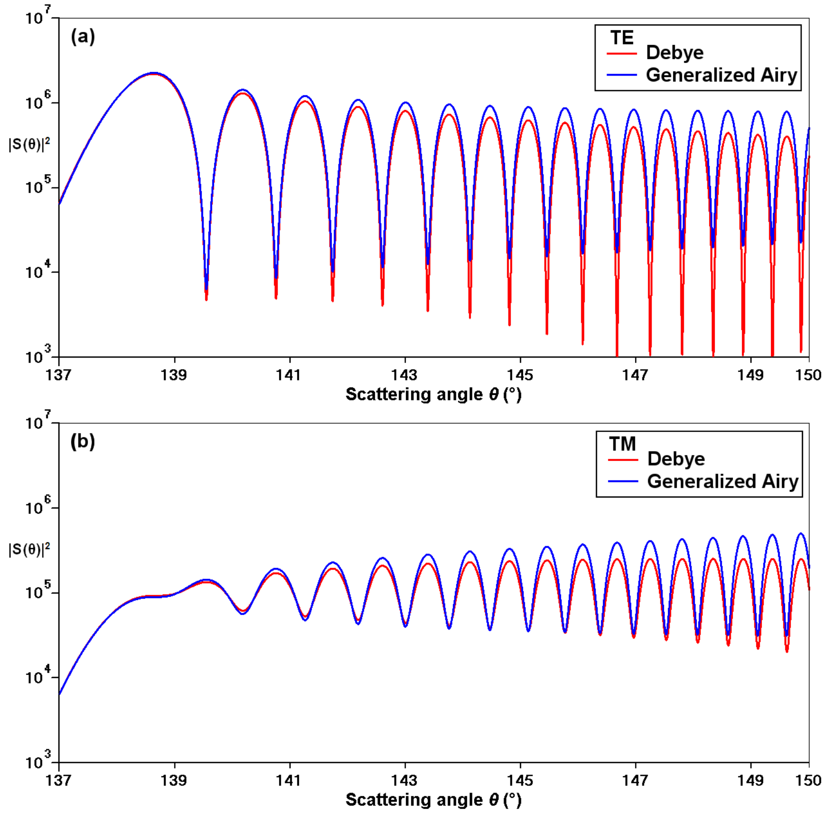

Fig. 6 As Fig. 5, except that a = 170 μm and x = 1,643. Spherical water drops having larger sizes than this evolve into oblate spheroids while falling.

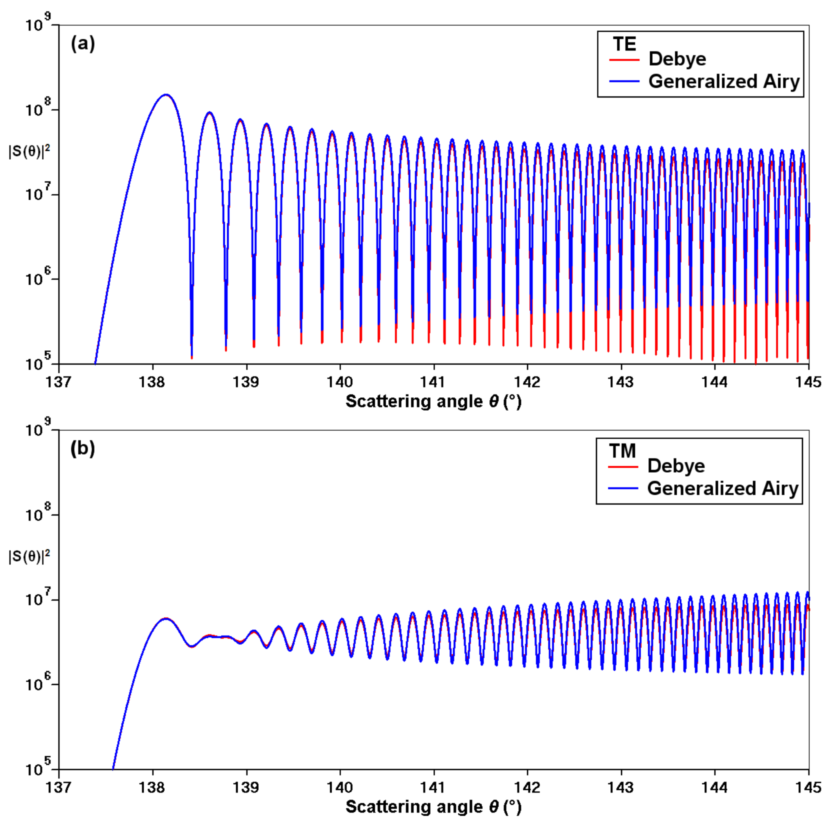

Fig.7 As Fig. 5, except that a = 1,034.5 μm and x = 10,000. The actual shapes of falling water drops of this size are highly distorted.

Figures 5-7 for $p = 2$, $N = 1.333$, $\lambda = 0.65$ µm, and $a = 37.24$ µm, 170 µm, and 1,035 µm, corresponding to $x = 360$, 1,643, and 10,000, respectively, show the scattered TE and TM intensity as a function of scattering angle for the exact Lorenz-Mie-Debye theory and generalized Airy theory of Eq. (3.29). As is easily seen, as x increases both the TE-polarized and TM-polarized generalized Airy theory intensity become an increasingly better approximation to the exact Lorenz-Mie-Debye theory intensity. In each figure, the results of Table 1 suggest that generalized Airy theory should be a valid approximation to exact Lorenz-Mie-Debye theory for the TE polarization in what we will call the angular interval of interest of the scattering angle, here $\theta \leq 140.81°$ (i.e., $\theta^R = 137.92°$ and $\Delta^{max} = 2.89°$ in Table 1. The size parameter considered in Fig. 5, $x = 360$, is the smallest for which Eq. (4.6) predicts that generalized Airy theory is a valid approximation to Lorenz-Mie-Debye theory for the TE polarization. The angular interval of interest encompasses the TE principal rainbow peak in Fig. 5. Although generalized Airy theory is not expected on the basis of Eq. (4.6) to closely approximate the TM-polarized Lorenz-Mie-Debye intensity until $x \approx 5{,}500$, the comparison is surprisingly good when x is as low as 360.

The size parameter considered in Fig. 6, $x = 1{,}643$, describes the nominal largest radius water drop that remains spherical as it falls for $\lambda = 0.65$ µm. The scattered intensity for the TE-polarized principal rainbow peak and the first supernumerary maximum now fall within the angular interval of interest, and again the comparison with the exact theory is quite good. The comparison for the TM-polarized intensity also remains quite good for this size parameter. For the size parameter considered in Fig. 7, $x = 10{,}000$, the first ten maxima of the TE-polarized supernumerary interference pattern now fall within the angular interval of interest. For the reasons described above, no false Brewster angle effect is observed in Fig. 7 at $\theta = 165.93°$.

For the TM polarization, both the true Brewster angle at $\theta^B = 138.74°$ and the nearby false Brewster angle at $\theta^{FB} = 138.53°$ lie slightly beyond the range of the TM angular interval of interest, which is now $\theta \leq 138.39°$. When $x = 1{,}643$ in Fig. 6, the Brewster angle artifact occurs in the vicinity of the reduced-height TM principal rainbow peak, and when $x = 10{,}000$ in Fig. 7, it has moved slightly past the first TM supernumerary maximum due to the angular narrowing of the rainbow and its supernumerary interference pattern as x increases. The angular position at which the generalized Airy theory intensity oscillations shift by 180° matches quite well with the angular location at which the 180° shift occurs in the exact Lorenz-Mie-Debye theory.

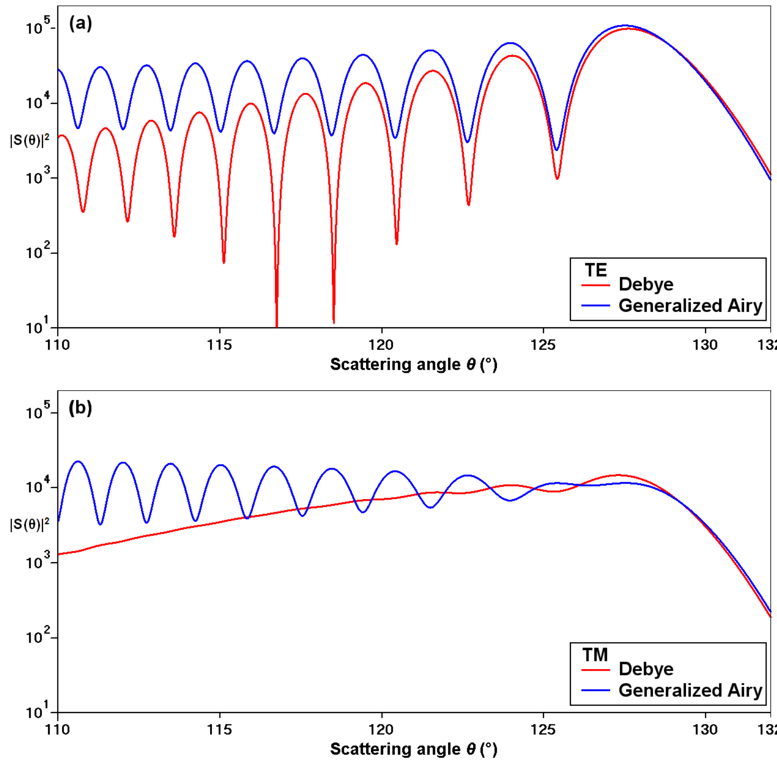

Fig. 8 Scattered intensity as a function of scattering angle for Lorenz-Mie-Debye theory and generalized Airy theory of Eq. (3.29) for (a) TE and (b) TM polarizations for $p = 3$, $N = 1.333$, $\lambda = 0.65$ μm, $a = 117$ μm, and $x = 1{,}130$. This is the smallest size parameter for which Eq. (4.6) predicts that generalized Airy theory is a valid approximation to Lorenz-Mie-Debye theory for the TE polarization.

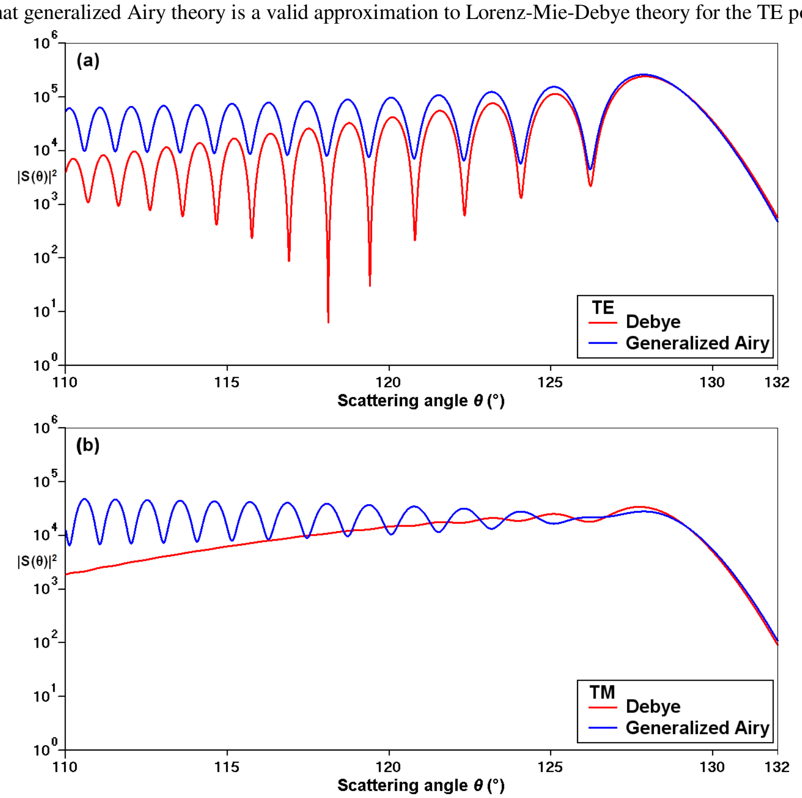

Fig. 9 As Fig. 8, except that $a = 170$ μm and $x = 1{,}643$. Spherical water drops having larger sizes than this evolve into oblate spheroids while falling.

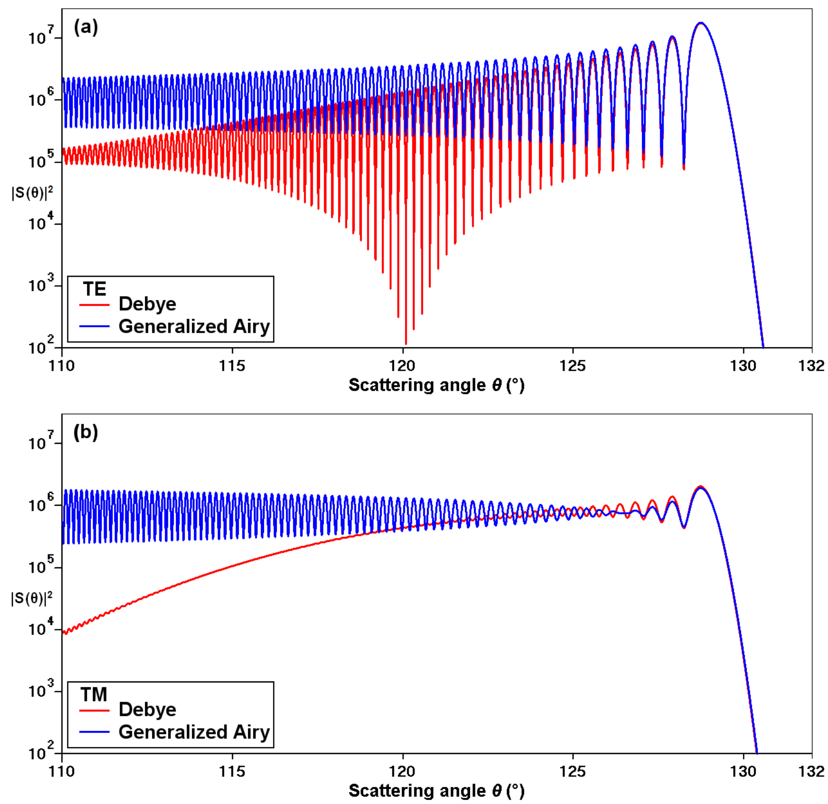

Fig. 10 As Fig. 8 except that a = 1,034.5 μm and x = 10,000. The shape of actual falling water drops of this size are highly distorted.

Figures 8-10 for $p = 3$, $N = 1.333$, $\lambda = 0.65$ μm, and a = 117 μm, 170 μm, and 1,035 μm, corresponding to x = 1,130, 1,643, and 10,000, respectively, show the scattered TE and TM intensity as a function of scattering angle, θ, for the exact Lorenz-Mie-Debye theory and generalized Airy theory of Eq. (3.29). The minima of the TE intensity of the exact theory are caused by the U and L rays being 180° out of phase with each other, with the deepest minima occurring at $\theta \approx 120°$ where the two rays have similar amplitudes. In each figure the results of Table 1 suggest that generalized Airy theory should be a valid approximation to Lorenz-Mie-Debye theory for the TE polarization in the angular interval of interest, which is now at the scattering angle $\theta \geq 126.68°$ (i.e., $\theta^R = 129.08°$and $\Delta^{max} = 2.40°$ in Table 1). The size parameter considered in Fig. 8, x = 1,130, is the smallest for which Eq. (4.6) predicts that generalized Airy theory is a valid approximation to Lorenz-Mie-Debye theory in the vicinity of the top of the principal TE rainbow peak.

The size parameter considered in Fig. 9, x = 1,643, again describes the nominal largest size water drop that remains spherical as it falls when $\lambda = 0.65$μm. The angular interval of interest now extends well past the principal rainbow peak, almost to the first supernumerary minimum. For x = 10,000 in Fig. 10, the angular interval of interest now extends past the third supernumerary maximum. Again, the comparison between generalized Airy theory TE intensity, and that of Lorenz-Mie-Debye theory is quite good in the angular region of interest, and it improves as x increases. But outside the angular interval of interest, $\theta < 126.68°$, the intensity of the relative minima of the supernumerary interference pattern of generalized Airy theory fails to reproduce the variations in the intensity of the supernumerary minima of Lorenz-Mie-Debye theory due to the U and L rays having similar amplitudes around $\theta \approx 120°$. The false Brewster angle artifact for the TE polarization at $\theta^{FB} = 111.52°$ does not occur, again for the reasons described in section 5.

The effect of the false Brewster angle artifact for the TM-polarized intensity so close to the Descartes rainbow angle, at $\theta^{FB} = 127.36$, is quite severe. Due to this artifact, the supernumerary oscillations of generalized Airy theory for the TM polarization quickly become 180° out of phase with the those of Lorenz-Mie-Debye theory for scattering angles beyond the generalized Airy theory angular interval of interest, which is now $\theta \geq 128.92°$ (i.e., $\theta^R = 129.08°$ and $\Delta^{max} = 0.16°$ in Table 1). This spurious 180° shift occurs in the vicinity of the principal TM rainbow peak in Fig. 8, at the first supernumerary minimum in Fig. 9, and at the fourth supernumerary minimum in Fig. 10.

The obvious lack of oscillations in the TM intensity of the exact theory in Figs. 8 - 10 is caused by the amplitude of the lower supernumerary ray being quite small over a large angular interval about the Brewster scattering angle $\theta^B = 115.01°$, so that the upper supernumerary ray is the dominant contribution to the scattered intensity.

7. Special Cases Beyond the Capability of Generalized Airy Theory

An interesting situation occurs for TM-polarized generalized Airy theory when $p = N^2$, so that the Descartes rainbow ray and the Brewster ray coincide. In this case, the coefficient of the Ai(-ζ) term of the TM polarization of generalized Airy theory is zero for $p = 2$, and the coefficients of both the Ai(-ζ) term and the Ai′(-ζ) term vanish for $p \geq 3$ [23]. Equation (3.29) can be written for the special case of $p = N^2$ as

$$\begin{aligned}\mathbf{E}_{\mathbf{scatt}}(r,\Theta,\varphi) \approx & [E_0 \exp(\mathrm{i}kr\text{-}\mathrm{i}\omega t)/(kr)] \exp(-\mathrm{i}p\pi/2) \exp(\mathrm{i}3\pi/4) \\ & \times \exp\{\mathrm{i}x[2pN \cos(\theta_t^R) - 2 \cos(\theta_i^R) + \Delta \sin(\theta_i^R)]\} \\ & \times x^{7/6} [(2\pi s)^{1/2} / h^{1/3}] [\sin(\theta)]^{-1/2} \\ & \times \{- \cos(\varphi)\, \mathbf{u}_\Theta\, \mathrm{i}\, h^{1/6} L_1 F^{TM\prime}(\theta_i^R)\, \mathrm{Ai}'(-\zeta) / x^{1/3} \\ & \quad + \sin(\varphi)\, \mathbf{u}_\varphi F^{TE}(\theta_i^R) [\mathrm{Ai}(-\zeta) + \mathrm{i}\, h^{1/6} M^{TE} \mathrm{Ai}'(-\zeta) / x^{1/3}]\} \ , \qquad (7.1)\end{aligned}$$

where L_1 was given in Eq. (2.14a), and

$$F^{TM\prime}(\theta_i^R) \equiv (\mathrm{d}F^{TM}/\mathrm{d}\theta_i)_R = 4pN^2hc^2 (2p^2N^2 - p^2 - N^4) (p - N^2)^{p-2} / (p + N^2)^{p+2} \qquad (7.2)$$

with the convention

$$\begin{aligned}(p - N^2)^{p-2} &= 1 \text{ if } p = 2 \\ &= 0 \text{ if } p \geq 3 \ . \qquad (7.3)\end{aligned}$$

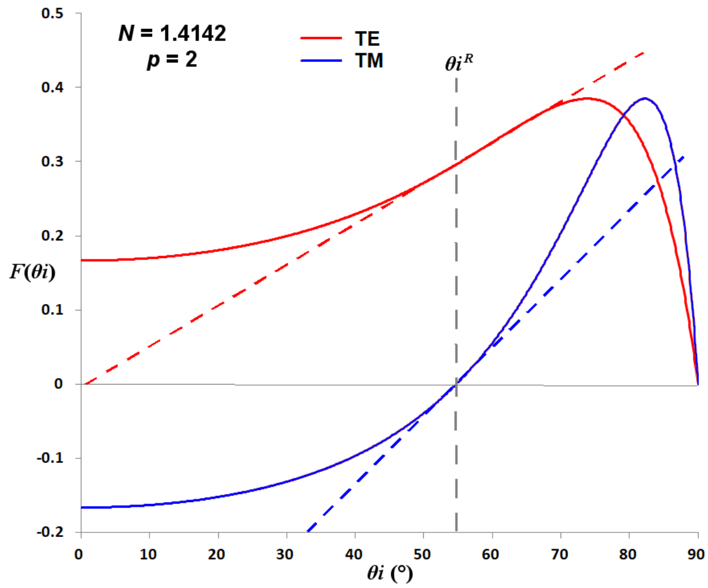

Fig. 11 Product of the TE and TM flat interface Fresnel coefficients as a function of the ray angle of incidence, $F^{TE}(\theta_i)$ and $F^{TM}(\theta_i)$, for transmission through a sphere following one internal reflection for $N = 1.4142$. The tangent to the curves at the angle of incidence of the Descartes rainbow ray, $\theta_i^R = 54.74°$, is also shown.

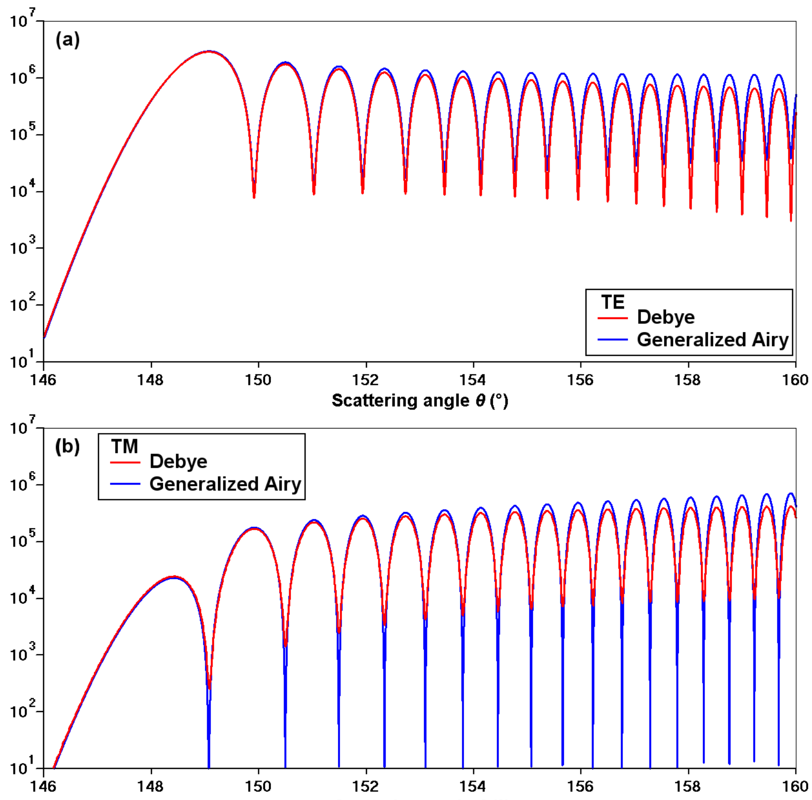

Fig. 12 Scattered intensity as a function of scattering angle for Lorenz-Mie-Debye theory and generalized Airy theory of Eq. (7.1) for (a) TE and (b) TM polarizations, $p = 2$, $N = 1.4142$, $\lambda = 0.65$ μm, $a = 155.2$ μm, and $x = 1{,}500$ where the Descartes rainbow ray and the Brewster angle ray coincide at $\theta^R = \theta^B = 148.41°$. The principal TM rainbow peak occurs very close to the Descartes rainbow scattering angle. The TM rainbow intensity is suppressed with respect to the TE rainbow intensity since the product of the Fresnel coefficients varies linearly about the Brewster ray.

Since the TM generalized Airy rainbow is described solely by Ai′(-ζ), for p = 2 and $N = 2^{1/2}$, The differential equation for the Airy integral (see Eq. (10.4.1) of [20]) can be used to show that the top of the principal TM rainbow peak should coincide with the Descartes rainbow scattering angle at $\zeta = 0$, or θ^R = 148.414°, rather than being shifted to ζ = -0.1088, as is the case for the TE rainbow which is dominated by Ai(-ζ). This is illustrated in Figs. 11 and 12 for p = 2, N = 1.4142, x = 1,500, where the top of the principal TM rainbow peak occurs at θ = 148.435° in Lorenz-Mie-Debye theory and at θ = 148.146° in generalized Airy theory. The peak intensity of the Lorenz-Mie-Debye TM rainbow for p = 2 and $N = 2^{1/2}$ is suppressed with respect to that of the TE rainbow because the product of the TM Fresnel coefficients in Fig. 11 vanishes at θ_i^R and varies linearly as a function of ε at the start of the supernumerary region. Fig. 12 shows that generalized Airy theory performs well in comparison with Lorenz-Mie-Debye theory, except that it underestimates the intensity of the TM minima.

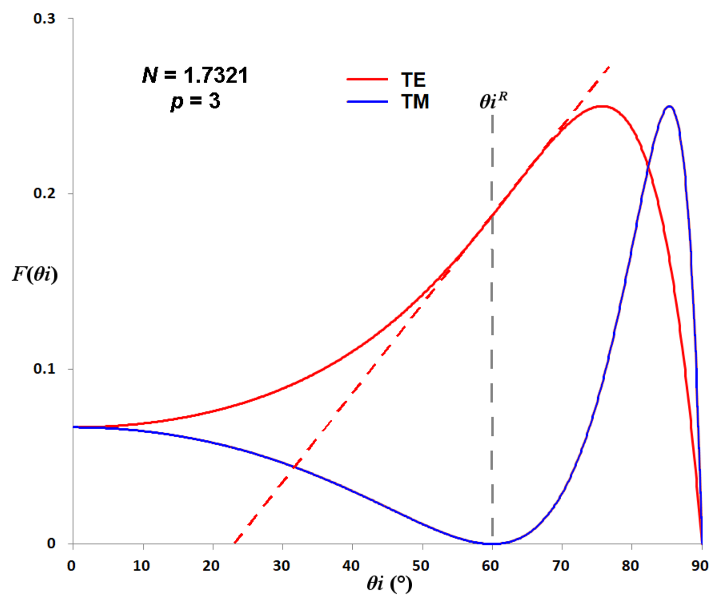

Fig. 13 Product of the TE and TM flat interface Fresnel coefficients as a function of the ray angle of incidence, $F^{TE}(\theta_i)$ and $F^{TM}(\theta_i)$, for transmission through a sphere following two internal reflections for N = 1.7321. The rainbow ray and the Brewster angle ray coincide at $\theta_i^R = \theta_i^B$ = 60.00°. The product of the TM Fresnel coefficients varies quadratically about that point.

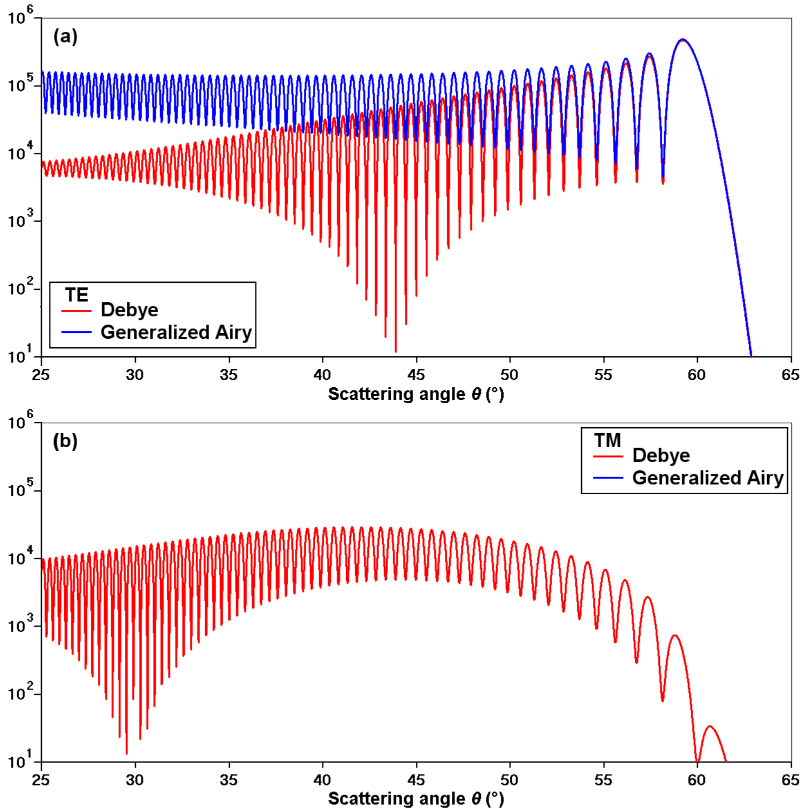

Fig. 14 Scattered intensity as a function of scattering angle for Lorenz-Mie-Debye theory and generalized Airy theory of Eq. (7.1) for (a) TE and (b) TM polarizations, $p = 3$, $N = 1.7321$, $\lambda = 0.65$ μm, $a = 155.2$ μm, and $x = 1{,}500$. Generalized Airy theory predicts zero scattered intensity for the TM polarization. The first TM supernumerary minimum for the exact Lorenz-Mie-Debye theory occurs very close to the Descartes rainbow scattering angle at $\theta^R = \theta^B = 60°$. The TM Lorenz-Mie-Debye rainbow intensity is further suppressed since the product of the Fresnel coefficients varies quadratically about the Brewster ray.

The case of $p = 3$ and $N = 3^{1/2}$ for TM polarization, shown in Figs. 13 and 14, lies beyond the capability of the generalized Airy theory we have described here since the coefficients of both Ai(-ζ) and Ai′(-ζ) in Eq. (7.1) are zero, resulting in the erroneous suppression of TM polarization in Fig. 14(b). A further generalization of Airy theory would allow Δ-dependence of the coefficient multiplying Ai(-ζ). [23] If this were to be the case, the scattered electric field would be proportional to $-\zeta\,\mathrm{Ai}(-\zeta)$. The top of the principal TM rainbow peak would occur when

$$\mathrm{Ai}(\zeta) + \zeta\,\mathrm{Ai}'(\zeta) = 0 \quad , \qquad (7.4)$$

which gives $\zeta \approx 0.88$ or $\theta = 60.7°$. The first supernumerary minimum would occur when $\zeta = 0$ or $\theta^R = 60.000°$. The prediction for the top of the principal rainbow peak compares favorably with the Lorenz-Mie-Debye theory result of Fig. 14 for $p = 3$, $N = 1.7321$, $x = 1{,}500$ where $\theta = 60.641°$. The prediction for the first supernumerary minimum also compares favorably with the Lorenz-Mie-Debye theory result of $\theta = 59.981°$. The suppression of the Lorenz-Mie-Debye TM rainbow for $p = 3$ and $N = 3^{1/2}$ is more severe than it was for $p = 2$ and $N = 2^{1/2}$ since the product of the Fresnel coefficients in Fig. 13 varies quadratically as a function of ε at the start of the supernumerary region. This suppression can be colloquially thought of as the Brewster angle effect eating a hole in the TM rainbow.

8. Conclusions

Airy's theory of the rainbow for scattering of a monochromatic plane wave by a single spherical particle is now almost two hundred years old. Although it is widely understood that it provides a very good qualitative understanding of many of the features of the rainbow, it is also widely believed to have some degree of difficulty in quantitatively describing the details of the scattered electric field. With the much more sophisticated light-scattering-based theories of the rainbow developed since then, people may easily wonder if there is anything new or useful left to say about Airy theory. This study has attempted to show that there is in fact much more to say about it. Lorenz-Mie-Debye theory exactly describes the $p \geq 2$ rainbows observed in light scattered by a spherical particle. But since the scattered electric field is the sum of the contribution of an infinite number of partial waves, the effects hidden within the theory are difficult to see in the structure of its equations. The original version of Airy theory assumed that all points on the wavefront exiting the sphere in the vicinity of the Descartes rainbow ray have a constant amplitude. As a result, it provides a simple but elegant first-order approximation to the exact results of Lorenz-Mie-Debye theory. On the other hand, the CAM-CFU approach uses the actual amplitude variation, and provides a high-level, but complicated, approximation. Since the generalized Airy theory studied here models the amplitude variation of the exiting wavefront in the vicinity of the Descartes rainbow ray by a linear function, it lies intermediate between the original version of Airy theory and the CAM-CFU uniform approximation. This gives it various advantages and disadvantages.

On the plus side, the introduction of the $\mathrm{Ai}'(-\zeta)$ term, multiplied by a constant coefficient, provides a much better fit to the exact results of Lorenz-Mie-Debye theory over a much broader range of sphere sizes than did the original version of Airy theory, with very little additional computational cost. For the TE polarization, $p = 2$, and $N = 1.333$ it was surprisingly found in [21] that the original version of Airy theory fit the exact results quite well for $x = 1{,}933$ and even $x = 483$, when van de Hulst's criterion [7] could not guarantee that the fit would be quantitatively accurate for $x < 5{,}000$. Generalized Airy theory allows one to explain and understand this in a natural way.

On the negative side, truncating the amplitude modeling of the outgoing wavefront at the linear term creates a false Brewster angle artifact in both the TE and TM polarizations. This turns out to be of no consequence for both the TE polarization and $N = 1.333$, and for the TM polarization, $p = 2$, and $N = 1.333$. However, the false Brewster angle artifact seriously corrupts the fit to the exact data for the TM polarization, $p \geq 3$, and $N = 1.333$, beginning almost immediately beyond what we have called the angular interval of interest, where the fit to the exact results is quite good.

In summary, Airy theory has long been considered to be a reasonably good qualitative approximation to the exact Lorenz-Mie-Debye results in the vicinity of the rainbow. Its generalization described here should raise its status to a quantitatively good approximation for the most commonly observed rainbow, namely $p = 2$, and the reasons for its serious shortcomings for $p \geq 3$ are now much better understood.

References

1. Boyer C.B. The Rainbow from Myth to Mathematics. Princeton NJ: Princeton U. Press; 1987.
2. Haußmann A. Rainbows in nature: recent advances in observation and theory. Eur. J. Phys. 2016; 37: 063001. https://doi.org/10.1088/0143-0807/37/6/063001
3. Laven P. Supernumerary arcs of rainbows: Young's theory of interference. Appl. Opt. 2017; 56: G104-G112. https://doi.org/10.1364/AO.56.00G104
4. Airy G.B. The intensity of light in the neighbourhood of a caustic. Trans. Camb. Phil. Soc. 1838; 6 part 3: 379-402.
5. Humphreys W.J. Physics of the Air. New York: Dover; 1964. Chapter 3.
6. Tricker R.A.R. Introduction to Meteorological Optics. New York: American Elsevier; 1970. Chapter 6, Appendix 1.
7. van de Hulst H.C. Light Scattering by Small Particles, New York: Dover; 1981.
8. Debye P. Das elektromagnetische Feld um einen Zylinder und die Theorie des Regenbogens Phys. Zeit. 1908; 9: 775-778. Reprinted and translated into English in Marston P.L., ed. Selected Papers on Geometrical Aspects of Scattering. SPIE Milestone Series vol. MS 89, 1994 Bellingham WA: SPIE Press; pp.198-204.
9. Nussenzveig H.M. High-frequency scattering by an impenetrable sphere. Ann. Phys. N.Y. 1965; 34: 23-95. https://doi.org/10.1016/0003-4916(65)90041-2
10. Nussenzveig H.M. High-frequency scattering by a transparent sphere: I. Direct reflection and transmission. J. Math. Phys 1969; 10: 82-124. https://doi.org/10.1063/1.1664764
11. Nussenzveig H.M. High-frequency scattering by a transparent sphere: II. Theory of the rainbow and the glory. J. Math. Phys 1969; 10: 125-176. https://doi.org/10.1063/1.1664747
12. Khare V., Nussenzveig H.M. Theory of the rainbow. Phys. Rev. Lett 1974: 33, 976-980. https://doi.org/10.1103/PhysRevLett.33.976
13. Nussenzveig H.M. Complex angular momentum theory of the rainbow and the glory. J. Opt. Soc. Am 1979; 69: 1068-1079, 1193-1194. https://doi.org/10.1364/JOSA.69.001068
14. Adam J.A. The mathematical physics of rainbows and glories. Phys. Rep. 2002; 356: 229-365. https://doi.org/10.1016/S0370-1573(01)00076-X
15. Chester C., Friedman B., Ursell F., An extension of the method of steepest descents. Math. Proc. Camb. Phil. Soc. 1957; 53: 599-611. https://doi.org/10.1017/S0305004100032655
16. Ursell F. Integrals with a large parameter. The continuation of uniformly asymptotic expansions. Proc. Camb. Phil. Soc. 1965: 61; 113-128. https://doi.org/10.1017/S0305004100038718
17. Berry M.V., Uniform approximation for potential scattering involving a rainbow. Proc. Roy. Soc. 1966: 89; 479-490. https://doi.org/10.1088/0370-1328/89/3/301
18. Connor J.N.L., Marcus RA., Theory of semiclassical transition probabilities for inelastic and reactive collisions. II. Asymptotic evaluation of the S matrix. J. Chem. Phys. 1971; 55: 5636-5643. https://doi.org/10.1063/1.1675732
19. Lee R.L. Mie theory, Airy theory, and the natural rainbow. Appl. Opt. 1998; 37: 1506-1519. https://doi.org/10.1364/AO.37.001506
20. Abramowitz M., Stegun I.A. Handbook of Mathematical Functions. Washington DC: National Bureau of Standards; 1964.
21. Wang R.T., van de Hulst H.C. Rainbows: Mie computations and the Airy approximation. Appl. Opt. 1991; 30: 106-117. https://doi.org/10.1364/AO.30.000106
22. Hovenac E.A., Lock J.A. Assessing the contributions of surface waves and complex rays to far-field Mie scattering by use of the Debye series. J. Opt. Soc. Am. A 1992; 9; 781-795. https://doi.org/10.1364/JOSAA.9.000781

23. Können G.P., de Boer J.H. Polarized rainbow. 1979. Appl. Opt. 1979; 18: 1961-1965. https://doi.org/10.1364/AO.18.001961
24. Pruppacher H.R., Beard K.V. A wind tunnel investigation of the internal circulation and shape of water droplets falling at terminal velocity in air. Quart. J. Roy. Met. Soc. 1970; 96; 247-256. https://doi.org/10.1002/qj.49709640807
25. Pruppacher H.R., Pitter R.L. A semi-empirical determination of the shape of cloud and rain drops. J. Atm. Sci. 1971; 28: 86-94. https://doi.org/10.1175/1520-0469(1971)028<0086:ASEDOT>2.0.CO;2
26. Zhang C., Rozé C., Ren K.F. Airy theory revisited with the model combining vectorial complex ray model and physical optics. Opt. Lett. 2022; 47: 2149-2152. https://doi.org/10.1364/OL.455940
27. Lock J.A., Laven P. The Debye Series and Its Use in Time-Domain Scattering 2016 in A. Kokhanovsky ed., Light Scattering Reviews, vol. 11. Berlin: Springer. https://doi.org/10.1007/978-3-662-49538-4
28. Born M., Wolf E., Principles of Optics, 6th ed. Cambridge, UK: Cambridge U. Press; 1980.
29. Möbius W. Zur Theorie des Regenbogens und ihrer experimentallen Prüfung. Abh. Kgl. Sachs. Ges. Wiss. Math-Phys. Kl. 1907-1909: 30: 105-254.
30. Möbius W. Zur Theorie des Regenbogens und ihrer experimentallen Prüfung. Ann. Phys. (Leipzig) 1910; 33: 1493-1558. https://doi.org/10.1002/andp.19103381622
31. Können G.P. Appearance of the supernumeraries of the secondary rainbow in rain showers. J. Opt. Soc. Am. A 1987; 4: 810-816. https://doi.org/10.1364/JOSAA.4.000810
32. Lock J.A., Können G.P. Rainbows by elliptically deformed drops: I. Möbius shift for high-order rainbows. Appl. Opt. 2017; 56: G88-G97. https://doi.org/10.1364/AO.56.000G88
33. Lock J.A. Supernumerary spacing of rainbows produced by an elliptical-cross-section cylinder: 1. Theory. Appl. Opt. 2000; 39: 5040-5051. https://doi.org/10.1364/AO.39.005040
34. Adler C.L., Phipps D., Saunders K.W., Nash J.K., Lock J.A. “Supernumerary spacing of rainbows produced by an elliptical-cross-section cylinder. 2. Experiment. Appl. Opt. 2001; 40: 2535-2545. https://doi.org/10.1364/AO.40.002535